

1. Report No. TX-00/3935-S		2. Government Accession No.		3. Recipient's Catalog No.	
4. Title and Subtitle Establishment of Reliable Methodologies to Determine In-Situ Moisture Content of Base and Subgrade Soils				5. Report Date July 1999	
				6. Performing Organization Code	
7. Author(s) Richard Liu, Xuemin Chen, Rong He, Wei Ma, Hongxu Wu				8. Performing Organization Report No. Project Summary Report 3935-S	
9. Performing Organization Name and Address Department of Electrical and Computer Engineering , University of Houston 4800 Calhoun Rd. Houston, TX 77204-4793				10. Work Unit No.	
				11. Contract or Grant No.	
12. Sponsoring Agency Name and Address Texas Department of Transportation Research and Technology Transfer Section, Construction Division P. O. Box 5080 Austin, TX 78763-5080				13. Type of Report and Period Covered Project Summary Report September 1997 – August 1998	
				14. Sponsoring Agency Code	
15. Supplementary Notes Project conducted in the cooperation with the Texas Department of Transportation					
16. Abstract:  <p>Pavement life span is often affected by the amount of voids in the base and subgrade soils, and especially by the soil moisture content. Time Domain Reflectometry (TDR) and Ground Penetrating Radar (GPR) are two desirable techniques to indirectly measure the in-situ soil moisture content through electrical properties of soils.</p> <p>The pre-purchased Tektronix 1502B TDR Cable Tester equipped with Campbell Scientific SDM1502 Communications Interface and PS 1502B Power Control Module system was successfully modified, installed, and integrated into the existing weather station in conjunction with the Texas Mobile Load Simulator (TxMLS) research project. The test sections were located on US281 near Jacksboro, Texas. The TDR results from US281 test sites indicated that the TDR sensors responded to the rainfall events favorably. The two-year field test results indicated that the TDR readings interpreted by Topp's (1980) and Ledieu's (1986) equations agreed well with the real measured value for the subgrade; none of the existing models for the base layers was found to be suitable for the soil moisture content conversion used in this research study. An empirical equation was established to determine the weight-based moisture content of the compacted base materials. Although the TDR system provides valuable information, it requires considerable time and effort to process data. In addition, the TDR system consumed too much power and caused malfunctions of the weather station. In that regard, a new Moisture Sensor (MS) system was developed in this study and verified at the Materials and Tests (MAT) section of TxDOT. The results from MAT section indicated that the MS system provides a more reliable solution than that of the TDR system. In addition, it is much easier to process the MS data. Furthermore, the MS system consumes almost no battery power and is an ideal solution for a long-term monitoring of pavement moisture content.</p> <p>Ground Penetrating Radar (GPR) was also employed at the same test sites. The Inversion Method was applied for converting moisture content of soils. Laboratory tests were satisfactory; yet the field application of this study needs further experiments to improve the results.</p>					
17. Key Words Volumetric/volume moisture content, gravimetric/weight moisture content, dielectric constant, Time Domain Reflectometry (TDR), Ground Penetrating Radar (GPR), inversion method, Moisture Sensor			18. Distribution Statement No restrictions. This document is available to the public through NTIS: National Technical Information Service 5285 Port Royal Road Springfield, Virginia 22161		
19. Security Classif. (of this report) Unclassified		20. Security Classif. (of this page) Unclassified		21. No. of Pages 70	22. Price



**Project Summary Report**

**ESTABLISHMENT OF RELIABLE METHODOLOGIES TO DETERMINE IN-SITU MOISTURE CONTENT OF BASE AND SUBGRADE SOILS**

Richard Liu (Research Supervisor)  
Xiemin Chen  
Rong He  
Wei Ma  
Hongxu Wu

Research Report 7-3935-S

Research Project 7-3935

Title: Establishment of Reliable Methodologies to Determine In-Situ Moisture Content of Base and Subgrade Soils

Conducted for the  
Texas Department of Transportation

**University of Houston  
4800 Calhoun Rd.  
Houston, Tx77204**

July 1999



## **DISCLAIMERS**

The contents of this report reflect the views of the authors, who are responsible for the facts and the accuracy of the data presented herein. The contents do not necessarily reflect the official views or policies of the Texas Department of Transportation. This report does not constitute a standard, specification or regulation.

There was no invention or discovery conceived or first actually reduced to practice in the course of or under this contract, including any art, method, process, machine, manufactory, design or composition of matter, or any new and useful improvement thereof, or any variety of plant, which is or may be patentable under the patent laws of the United States of America or any foreign country.

## **ACKNOWLEDGMENTS**

The authors would like to express their sincere appreciation to Dr. Dar-Hao Chen, P.E., and Dr. Mike Murphy, P.E., for their assistance and guidance. Thanks are expressed to Mr. Cy Helms, Mr. John Bilyeu and Dr. Andrew Wimsatt, P.E., for their assistance during installation of the TDR system. Also, thanks are expressed to Dr. Wei Wu, P.E., Dr. James Lee, P.E., and Mr. John Bilyeu for their input and comments in preparation of this project summary report.

Richard Liu, Ph.D., P.E.

Research Supervisor

## **ABSTRACT**

Pavement life span is often affected by the amount of voids in the base and subgrade soils and especially by the soil moisture content. Time Domain Reflectometry (TDR) and Ground Penetrating Radar (GPR) are two desirable techniques to indirectly measure the in-situ soil moisture content through electrical properties of soils.

The pre-purchased Tektronix 1502BTDR Cable Tester equipped with Campbell Scientific SDM1502 Communications Interface and PS 1502B Power Control Module system was well modified, installed, and integrated into the existing weather station in conjunction with the Texas Mobile Load Simulator (TxMLS) research project. The test sections were located on US281 near Jacksboro, Texas. The TDR results from US281 test sites indicated that the TDR sensors responded to the rainfall events favorably. The two-year field test results indicated that the TDR readings interpreted by Topp's (1980) and Ledieu's (1986) equations agreed well with the real measured value for the subgrade. However, none of the existing models for the base layers was found to be suitable for the soil moisture content conversion used in this research study. An empirical equation was established to determine the weight-based moisture content of the compacted base materials. Although the TDR system provided valuable information, it required considerable time and effort to process data. In addition, the TDR system consumed too much power and caused malfunctions of the weather station. Accordingly, a new moisture sensor (MS) system was developed in this study and verified at the Materials and Tests (MAT) section of TxDOT. The results from MAT section indicated that the MS system provides a more reliable solution than the TDR system. In addition, it is much easier to process the MS data. Furthermore, the MS system consumes almost no battery power and is an ideal solution for long-term monitoring of pavement moisture content.

Ground Penetrating Radar (GPR) was also employed at the same test sites. The Inversion Method was applied for calculating moisture content of the soils. Laboratory tests were satisfactory; yet the field application of this study needs further experimentation to improve the test results.

## **IMPLEMENTATION RECOMMENDATIONS**

This research project assists TxDOT to install, calibrate, and monitor the TDR system that was purchased under Texas Mobile Load Simulator (MLS) operation budget. The TDR system was purchased three years prior to this research project. Although the TDR system provided valuable information, it required much time and effort to process the data. Also, the TDR system consumed much power from the remote weather station. The weather station has been down twice due to lack of power from the battery. With advances in technology, hardware and software can be developed to monitor the in-situ moisture content reliably and economically. According, a new moisture content measurement system has been devised in this study. This developed Moisture Sensor (MS) system has been verified at the Soil and Aggregate Branch of the Materials and Tests (MAT) section of TxDOT. The test results from the MAT section indicated that the MS system provided an accurate and reliable solution. In addition, the MS system offers a much easier way to process the data. Furthermore, the power consumption rate of MS is so low that it consumes almost no energy from the battery.

Specific approaches to implement the MS system are as follows:

- 1) Install the MS system in a trial section. The MLS test site is the best candidate section because it possesses the weather station on-site. The in-situ moisture content data can be related to the rainfall data as well as the FWD results. The effects of the variation of moisture content on the pavement can be derived from the result of the FWD tests.
- 2) Bring the soil from the test site and measure its moisture content in a laboratory to compare with the result from the MS system.
- 3) After long-term monitoring or several iterations of 1) and 2), a guideline for in-situ moisture content measuring can be developed.
- 4) The guideline from 3) will assist other research projects or special construction projects that require in-situ moisture content data.





## TABLE OF CONTENTS

ABSTRACT .....	vi
IMPLEMENTATION RECOMMENDATIONS .....	vii
LIST OF FIGURES .....	xi
LIST OF TABLES .....	xiii
CHAPTER 1: INTRODUCTION .....	1
1.1 PROJECT OVERVIEW .....	1
CHAPTER 2: LITERATURE REVIEW .....	3
2.1 TIME DOMAIN REFLECTOMETRY BACKGROUND .....	3
2.2 COMPONENTS OF TDR SYSTEM.....	4
2.3 SIMULATION OF WAVEFORM REFLECTED FROM THE TDR PROBE: AN ALGORITHM FOR DETERMINATION OF SOIL MOISTURE CONTENT .	5
CHAPTER 3: TDR SYSTEM.....	7
3.1 THEORY OF TDR METHOD .....	7
3.2 VOLUME AND WEIGHT MOISTURE CONTENT RELATION .....	8
CHAPTER 4: FIELD TEST RESULTS OF THE TDR SYSTEM .....	15
4.1 TEST SECTION .....	15
4.2 TEMPERATURE VARIATION AND SUBSURFACE MOISTURE MOVEMENT.....	16
4.3 TDR INSTALLATION PROFILE.....	17
4.4 TDR INTERPRETATION METHODS AND TEST RESULTS .....	18
4.4.1 Interpretation Method for Base Layer .....	19
4.4.2 Interpretation Methods for Subgrade .....	19
4.4.3 Field Test Results .....	20
CHAPTER 5: GPR SYSTEM: ITS IMPLEMENTATION AND TEST RESULTS.....	27
5.1 BACKGROUND OF GPR TECHNIQUE.....	27

5.1.1 Inversion Method .....	27
5.2 COMPONENTS OF GPR SYSTEM .....	30
5.3 GPR SYSTEM TEST SET-UP .....	30
5.3.1 Laboratory Test Set-Up .....	30
5.3.2 Field Test Set-Up .....	31
5.4 GPR DATA PROCESSING.....	31
5.4.1 Basic Procedure.....	31
5.4.2 Inversion Results of Synthetic Data .....	32
5.4.3 Inversion Results of Field Data .....	32
5.5 TEST RESULTS .....	33
5.5.1 Laboratory Test Results .....	33
5.5.2 Field Test Results .....	34
CHAPTER 6: CONCLUSIONS.....	37
6.1 TDR SYSTEM .....	37
6.2 GPR SYSTEM .....	37
CHAPTER 7: RECOMMENDATIONS .....	39
7.1 THE NEW MOISTURE CONTENT MEASUREMENT SYSTEM.....	39
7.1.1 The Basic Principle of the New Moisture Sensor .....	39
7.1.2 Laboratory Tests at UH .....	41
7.1.3 Laboratory Tests at TxDOT Materials Lab .....	43
APPENDIX .....	45
A.1 SYSTEM I: SYSTEM FOR THE LABORATORY MEASUREMENT OF SOIL MOISTURE CONTENT .....	45
A.2 SYSTEM II: SYSTEM FOR THE IN-SITU MEASUREMENT OF SOIL MOISTURE CONTENT .....	45
A.3 TDR HARDWARE SYSTEM .....	45
A.3.1 Introduction of the System .....	45
A.3.2 Hardware Components .....	46
A.4 SOFTWARE TOOLS.....	48
REFERENCES.....	53

## LIST OF FIGURES

Figure 2.1 The Tektronix 1502B TDR cable tester.....	4
Figure 2.2 Schematic of TDR measurement system.....	5
Figure 2.3 Ideal waveform reflected under strictly resistive impedance .....	6
Figure 2.4 Actual waveform reflected from the TDR probe.....	6
Figure 3.1 Volume and weight moisture contents relation .....	11
Figure 3.2 Weight and volume moisture contents relation using soil dry density .....	11
Figure 3.3 Weight moisture content $W_w$ (%) vs. volume moisture content $W_v$ (%) under different compactions.....	13
Figure 4.1 Pavement sections of southbound and northbound US281 .....	16
Figure 4.2 Temperature variations at a depth of 88.9 mm .....	17
Figure 4.3 Southbound US281, TDR sensor installation profile .....	18
Figure 4.4 Rainfall and $W_w$ for southbound TDR #4 in the base layer (0.368 m).....	23
Figure 4.5 Rainfall and $W_w$ for southbound TDR #3 in the subgrade layer (1.02 m).....	24
Figure 4.6 Rainfall and $W_w$ for southbound TDR #5 in the subgrade layer (0.686 m).....	25
Figure 4.7 Rainfall and $W_w$ for southbound TDR #8 in the subgrade layer (0.914 m).....	26
Figure 5.1 A block diagram of a GPR system used in the moisture content measurement.....	29
Figure 5.2 An N-Layer information profile (left (top) → right (bottom)) .....	29
Figure 5.3 Sand box with two layers of sand of different moisture contents.....	31
Figure 5.4 Inversion result using synthetic data.....	32
Figure 5.5 Waveform of the direct wave.....	34
Figure 5.6 A trace from the two-layer sand sample .....	34
Figure 7.1 The new moisture content measurement system: a) The MS probe b) The MS main system c) Lab test at UH d) Soil sample test .....	39
Figure 7.2 A two-wire transmission line diagram.....	40
Figure 7.3 The cross-section of the sensor .....	40
Figure 7.4 Phase vs. weight moisture content.....	43
Figure A1 Schematic of the modified CR10 datalogger for the TDR system .....	46
Figure A2 Wiring diagram of the multiplexer communication cables from the SDM1502 and SDM50 to the datalogger.....	49

Figure A3 Datalogger wiring for the TDR (left part of this figure is the thermocouples installed at US281, Jacksboro, Texas) ..... 50

Figure A4 Program flow chart ..... 51

## LIST OF TABLES

Table 3.1 Dielectric constant $\epsilon$ for typical construction materials .....	8
Table 3.2 Typical values of void ratios and dry unit weights for granular soils .....	9
Table 3.3 Weight moisture content vs. volume moisture content – measured data .....	12
Table 3.4 A summary of some existing empirical models .....	13
Table 4.1 The overall evaluation of the 8 TDRs at southbound US281 test site .....	21
Table 4.2 The overall evaluation of the 8 TDRs at northbound US281 test site .....	21
Table 4.3 TDRs monthly average $W_w$ (%) for southbound US281 test site .....	21
Table 4.4 TDRs monthly average $W_w$ (%) for northbound US281 test site .....	22
Table 5.1 Background knowledge for southbound US281, Jacksboro, Texas .....	31
Table 5.2 Inversion results when sampling rate is 50 ps .....	33
Table 5.3 Inversion results when sampling rate is 100 ps .....	33
Table 5.4 Comparison of the one-layer sand real moisture content and the GPR result ..	35
Table 5.5 Comparison of the two-layer sand real moisture content and the GPR result ..	35
Table 7.1 Data measured during two experiments for sand and soil samples .....	42

# CHAPTER 1: INTRODUCTION

## 1.1 PROJECT OVERVIEW

There are many methods to measure soil moisture content. In the past, the gypsum block and nuclear gage method were used to measure in-situ moisture content. Several methods such as the sand-cone method, drive-cylinder method, and rubber-balloon method are available for measuring the in-situ density of soil, which in turn can estimate the moisture content. Nevertheless, these methods are not sufficient to measure the moisture content in an accurate, fast, safe and non-destructive manner. The Time Domain Reflectometry (TDR) and Ground-Penetrating Radar system (GPR) are two methods favorable to the purpose. Although the use of TDR and GPR theories to indirectly measure the in-situ volumetric moisture content of soil are not new, the implementation of these techniques is fairly new. TxDOT would like to monitor the moisture content variation of the MLS test sites using the TDR system which had been purchased 3 years before. This research project has focused on the following tasks:

- 1) Modifying the pre-purchased TDR device by adding a datalogger (CR10) which was an automatic data acquisition system from the existing weather station;
- 2) Assisting TxDOT with calibration and integration of the TDR system into the existing weather station;
- 3) Investigating suitable equations to convert the dielectric constant to weight-based moisture content for granular material and subgrade soils; and
- 4) Devising an ideal long-term moisture measurement device, the Moisture Sensor (MS) system, for the MLS project and other research projects or special construction projects that require in-situ moisture content data.

Also, a Ground Penetration Radar (GPR) method has been investigated in order to compare the test results from different methods. The EKKO1000 GPR system manufactured by Sensors & Software Corp. was employed, and an inversion method was proposed to analyze the field data acquired from highway US281 in Jacksboro, Texas. However, at the current stage, the field test results from GPR are not satisfactory.



## CHAPTER 2: LITERATURE REVIEW

### 2.1 TIME DOMAIN REFLECTOMETRY BACKGROUND

The Time Domain Reflectometry (TDR) technique was originally developed to locate faults in communication cables. In the 1950s, it was adopted by the agricultural community to measure soil moisture content [1]. The TDR technique is based on detecting the change in impedance at the media interfaces. The change in impedance causes part of the electromagnetic pulse to be reflected. The dielectric constant  $\epsilon$  of a medium is a complex value and can be expressed as  $\epsilon = \epsilon' - j * \sigma / \omega$ . In this report,  $\epsilon'$  is the real part and  $\sigma / \omega$  is the imaginary part, where  $\sigma$  is the conductivity of the soil and  $\omega$  is the angular frequency of the measurement system. A detailed explanation of this equation is described in Chapter 3. For most soils, studies show that the complex value of dielectric constant strongly depends on the real part when the frequencies of electromagnetic pulses are in the range of 1 MHz to 2 GHz, which is contributed by soil moisture content. Because the dielectric constant of free water is at least 15 times higher than that of most soils under dry conditions, the moisture content can be determined from the reflected signal of electromagnetic pulses. The contribution of the imaginary component of the dielectric can be ignored when compared to the real part. Many researches, mostly in soil science, have been done to develop TDR technology to measure soil moisture content.

Initially, TDRs for measuring soil moisture content used coaxial transmission lines (Topp et al. 1980). Later, it was found in field applications that coaxial transmission lines are inappropriate for this type of installation. Two-rod parallel transmission lines were substituted and used to monitor field moisture contents (Topp et al. 1982, 1984, 1985). The two-rod parallel transmission lines achieved limited success, because they needed impedance-matching transformers, which tended to distort the shape of the signal. Generally speaking, a multiple-rod probe can better simulate coaxial transmission lines and does not require the use of a balancing transformer. However, it was found that with an increase in number of rods, the installation difficulty and soil disturbance also increase. In field operations, the optimum setup is a three-rod probe transmission lines TDR cable tester. A three-rod probe TDR cable tester achieved the following desirable features: signal clarity, ease of installation and stability. Many researchers, such as Kotdawala et al. (1994), Rada et al. (1994), and Schelt et al. (1994) [1-2], have successfully used a three-rod probe TDR cable tester for measuring in-situ moisture content of soils. Figure 2.1 shows a picture of the Tektronix 1502B TDR three-rod probe cable tester.

There are balanced and unbalanced arrangements for the probes within three-rod probe TDR cable testers. The advantages for an unbalanced probe are: 1) they are smaller than with the balanced design in size; and 2) the measurement is concentrated around the central electrode. The Tektronix 1502B is an unbalanced probe cable tester employed in this project.



To date, most of the field applications of TDR systems are still for monitoring moisture content on a long-term basis. This design is not suitable for repeated installation. In this research project, the modified one-time installation TDR probes provide adequate accuracy in both laboratory and field environments. However, the data processing requires well-trained professionals. These probes are also relatively expensive because of their size and energy consumption.

A brand-new moisture content measurement system was developed by the research team and verified at the Materials and Tests (MAT) section of TxDOT. This small, simple, low-cost, energy-saving, and high-accuracy Moisture Sensor (MS) system will overcome the disadvantages of the current modified TDR system. The development of the MS system is presented in Chapter 7.

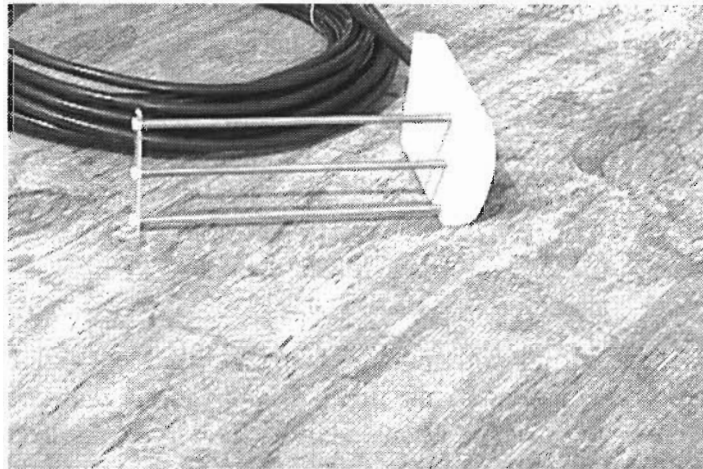


Figure 2.1 The Tektronix 1502B TDR cable tester

## 2.2 COMPONENTS OF TDR SYSTEM

A TDR instrument is basically composed of a pulse generator and an oscilloscope. The pulse generator sends an electrical pulse along the cable link, and the oscilloscope is used to observe the returning echoes. The simplest TDR probe consists of two or three parallel rods inserted into the soil. These rods are attached directly to a twin-lead cable, and the other end of the cable is connected directly to the front panel of the Time-Domain Reflectometry unit. Figure 2.2 is a simplified schematic of the Time-Domain Reflectometry unit 1502B.

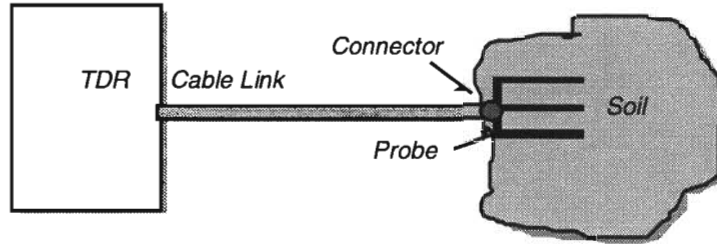


Figure 2.2 Schematic of TDR measurement system

### 2.3 SIMULATION OF WAVEFORM REFLECTED FROM THE TDR PROBE: AN ALGORITHM FOR DETERMINATION OF SOIL MOISTURE CONTENT

Based on Ledieu's study, a simplified linear relationship between dielectric constant and the soil moisture content is developed and is given in Eq. (3.5) in Chapter 3. A similar relationship was also reported by Topp et al. (1980) and Liu et al. [3][4-6].

The step function has a very wide frequency range, and a theoretical explanation for this is given in Chapter 3. Generally, when the frequency is above 500 MHz, the complex dielectric constant of soil primarily depends on the moisture content of the soil. However, when the frequency is under 500 MHz, the complex dielectric constant of the soil is a function of both the moisture content and the frequency [7-8]. Permittivity of the probe decreases with the frequency, and the conductivity increases with the frequency [9-10]. The impedance of the probe is a function of the frequency. Resistance and conductance of the probe are also functions of the frequency. For line aberrations that are strictly resistive, any reflection looks like a portion of the incident voltage. Figure 2.3 shows the waveform reflected in this ideal situation. In an actual reflected waveform, the frequency of a waveform is a complex frequency, and the impedance is complex impedance. Figure 2.4 shows an actual reflected waveform.

The reflected waveform is calculated using the Fourier analysis. The reflectivity at the points of impedance discontinuity along the TDR probe is added to form the whole waveform [11].

To determine soil moisture content by analyzing the reflected waveform from the TDR probe, the two rising (or falling) edge arrival times of the reflected waveform from the two ends of the probe must be identified from the reflected waveform. In this report, an algorithm is developed based on the simulation results. Two systems are developed for different purposes. System I is developed for laboratory study and System II is developed for field measurement. The details of both systems are addressed in the appendix.

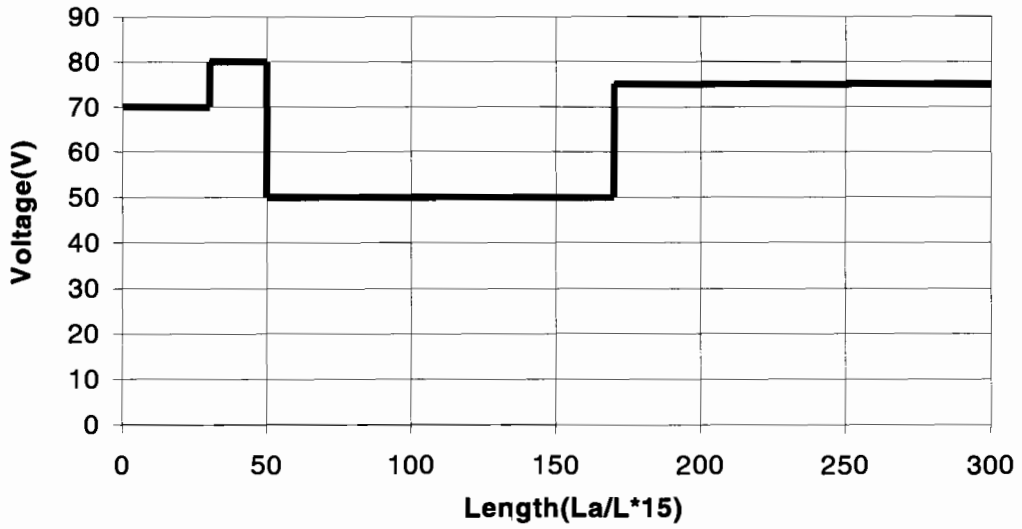


Figure 2.3 Ideal waveform reflected under strictly resistive impedance

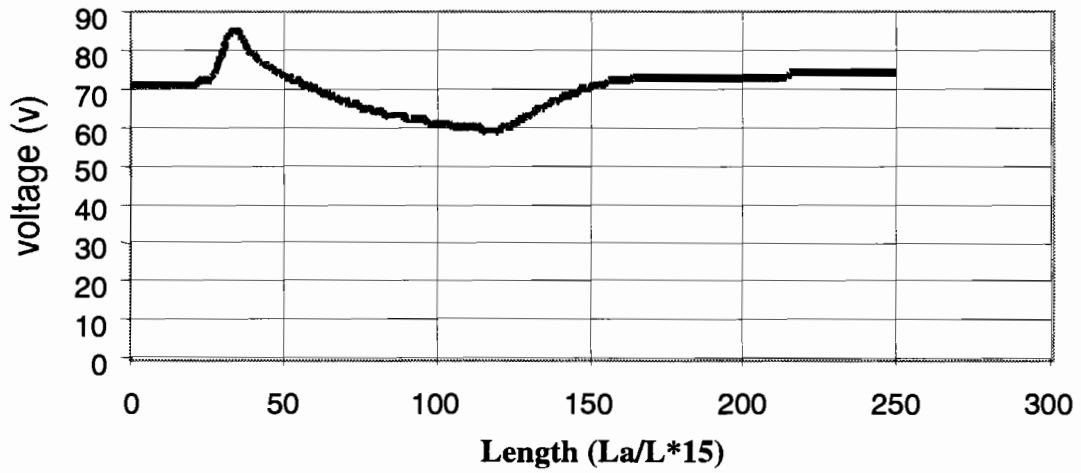


Figure 2.4 Actual waveform reflected from the TDR probe

## CHAPTER 3: TDR SYSTEM

### 3.1 THEORY OF TDR METHOD

The process of sending pulses and observing the reflected waveforms is called the Time Domain Reflectometry (TDR) technique. TDR was originally used to determine the location of failure in telecommunication cables, as well as to measure the velocity of electromagnetic waves travelling through a transmission line. This velocity ( $v$ ) is related to the dielectric constant  $\epsilon$  of the insulating medium between the conductors of the transmission line given by:

$$v = c / \sqrt{\epsilon} \quad (3.1)$$

where  $c$  is the velocity of light in vacuum, which is a constant of 30 cm/nsec (300,000 km/s or 11.8 in/nsec) and  $\epsilon$  is the dielectric constant of the medium. A TDR probe used to measure soil moisture content is actually a transmission line, and the dielectric medium is the surrounding soil. In practice, the  $c$  value is often slightly different from the theoretical value, because the medium is not a vacuum. The difference of  $c$  values in different media is so small that from a practical viewpoint it can either be simply ignored, or the calculation can be performed using a modified value. Thus, the relationship between the propagation velocity of electromagnetic waves and the dielectric constant of the medium in which the wave is propagating becomes very simple. If the dielectric constant of the layer is known, the velocity can be determined.

A phase lag exists due to the constituent molecules or dipolar species when electromagnetic waves propagate through an imperfect dielectric medium. Because of this phase lag, dielectric constant must be represented as a complex quantity  $\epsilon$ :

$$\epsilon = \epsilon' + \epsilon'' \quad (3.2)$$

where  $\epsilon'$  is the real part (in phase),  $\epsilon''$  is the imaginary part (out of phase), and  $\epsilon''$  can be expressed as:

$$\epsilon'' = -j * \sigma / \omega \quad (3.3)$$

where  $\sigma$  is the conductivity of the soil, and  $\omega$  is the angular frequency of the measurement system. By combining Eqs. (3.2) and (3.3), the dielectric constant  $\epsilon$  can be expressed as:

$$\epsilon = \epsilon' - j * \sigma / \omega \quad (3.4)$$

TDR measures the apparent dielectric constant  $\epsilon$ , which depends on both the frequency of the TDR signal and the conductivity of the soil. When the operating frequency is high, usually above 500 MHz, the weight of the imaginary part is negligible. However,  $\epsilon'$  appears to be more sensitive to the volume moisture content ( $W_v$ ) and less sensitive to the soil type and density [3,12]. For a given soil, the response of a TDR's receiver to an electromagnetic excitation is thus a function of free-water moisture content, because the dielectric constant of the free-water is much greater than that of the dry soil. Table 3.1 lists typical values of the dielectric constant  $\epsilon$  for materials often encountered in

highway conditions. The extremes of these values are for air  $\epsilon_{air} = 1$ , and for water  $\epsilon_{water} = 81$  [13].

*Table 3.1 Dielectric constant  $\epsilon$  for typical construction materials [13]*

<b>Material</b>	<b>Dielectric Constant <math>\epsilon</math></b>
Vacuum / Air	1
Water	81
Sand (dry)	4~6
Sand (wet)	30
Silt (wet)	10
Clay (wet)	8~12
Ice (fresh)	4
Granite (dry)	5
Limestone (dry)	7~9
Portland Cement Concrete	6~11
Roller-Compacted Concrete	5~7
Asphaltic Concrete	5~7

### 3.2 VOLUME AND WEIGHT MOISTURE CONTENT RELATION

Many researchers have developed different models relating the moisture content and dielectric constant of soil. Among those models, Ledieu et al. (1986), Topp et al. (1980) and a method of Simple Lattice (which is based on a theoretical computation) all agree with each other and give good results for subgrade soils. The theoretical method is not presented in this report [14].

In the datalogger programming, a multiplier of 0.1138 and an offset -0.1758 give volume / volumetric moisture content (Ledieu) in terms of dielectric constant:

$$W_v = 0.1138\sqrt{\epsilon} - 0.1758 \quad (3.5)$$

where  $W_v$  is the volume / volumetric moisture content and  $\epsilon$  is the dielectric constant.

In the field of civil engineering, the weight (gravimetric) moisture content  $W_w$  is more frequently used than the volume (volumetric) moisture content  $W_v$ . Weight moisture content is defined as:

$$W_w = \frac{W_{water}}{W_{soil}} \quad (3.6)$$

where  $W_w$  is the weight moisture content of the soil,  $W_{water}$  is the weight of water in the soil and  $W_{soil}$  is the weight of the soil particles.

Theoretically speaking, the relation between the two parameters is:

$$W_v = W_w * (\rho / \rho_{water}) \quad (3.7)$$

where  $\rho$  is the wet soil density (unit weight) and  $\rho_{water}$  is the water density (unit weight). Figure 3.1 shows the relationship between the volume and weight moisture content when wet density  $\rho$  is known.

With known dry density  $\rho_{dry}$  (in most cases) and the assumption of zero air weight, Eqs. (3.8) and (3.9) can be constructed to related  $W_v$  to  $W_w$ .

$$\rho = \frac{W}{V_{total}} = \frac{W_{soil} + W_{water}}{V_{total}} = \frac{W_{soil} + \rho_{water} * V_{water}}{V_{total}} = \rho_{dry} + W_v * \rho_{water} \quad (3.8)$$

$$W_v = \frac{W_w}{1 - W_w} * (\rho_{dry} / \rho_{water}) \quad (3.9)$$

Table 3.2 lists the typical values of void ratios and dry unit weights for granular soils [15]. The curves in Figures 3.1 and 3.2 are based on the typical range of dry unit weight for granular soils in Table 3.2. Comparing Figure 3.1 with Figure 3.2, one can find that these two formulas give very close results when the weight moisture content of the soil is small compared to the dry density; or  $W_w \ll \rho_{dry}$ . For a typical soil, the weight moisture content  $W_w$  is about 0.15, and the density is 1.5 g/cm<sup>3</sup> (93.6 pcf). Using Eq. (3.7), the volume moisture content  $W_v$  is 0.23, and using Eq. (3.9) the volume moisture content  $W_v$  is 0.26, assuming the same value of 1.5 g/cm<sup>3</sup> (93.6 pcf) for both  $\rho$  and  $\rho_{dry}$ .

*Table 3.2 Typical values of void ratios and dry unit weights for granular soils [15]*

Soil type	Void ratio e		Dry unit weight $\rho_{dry}$			
	Maximum	Minimum	Minimum		Maximum	
			lb/ft <sup>3</sup>	KN/m <sup>3</sup>	lb/ft <sup>3</sup>	KN/m <sup>3</sup>
Gravel	0.6	0.3	103	16	127	20
Coarse sand	0.75	0.35	95	15	123	19
Find sand	0.85	0.4	90	14	118	19
Standard Ottawa sand	0.8	0.5	92	14	110	17
Gravelly sand	0.7	0.2	97	15	138	22
Silty sand	1	0.4	83	13	118	19
Silty sand and gravel	0.85	0.15	90	14	144	23

The TDR system modified in this study was intended to measure the moisture content of the pavement's base layer and the subgrade. Unlike the natural soil, base materials are

often compacted by mechanical force, which leads much higher densities than with un-compacted subgrade soils. The “natural” structures of the materials have been disturbed. Recent studies such as by Roth et al. (1992) and Zegelin et al. (1992) found that some of the “universal” empirical models like Topp’s equation did not provide sufficiently accurate results for soils of too high densities [1-2]. Experimental work was conducted in this study to support the above conclusion, and a new relationship is established between the dielectric constant and the weight moisture content of base layer materials (or compacted soils). The soil samples were obtained from the southbound lanes of US281, Jacksboro, Texas. A standard compactor was used to compact the soil samples during this experiment. From Eq. (3.7), it is easy to note that there is no unique relationship between the weight moisture content  $W_w$  and the volume moisture content  $W_v$ , because the soil density  $\rho$  is a variable. One weight moisture content  $W_w$  may correspond with different volume moisture contents  $W_v$  under different compaction efforts. The volume moisture content  $W_v$  and weight moisture content  $W_w$  obtained in this study are listed in Table 3.3 and plotted in Figure 3.3. In Table 3.3, low compaction means no mechanical effort, the number of blows is 0 and the density of the soil is approximately 85 pcf. Medium compaction means the number of blows is 100 and the density of the soil is approximately 120 pcf. High compaction means the number of blows is 300 and the density of the soil is approximately 141 pcf. Table 3.4 summarizes some of the existing empirical models. Obviously, the existing empirical models in Table 3.4 [1] are not suitable for TDR interpretation of base materials, because the relationship relating to the compacted condition is not reflected in any one of the above researches, except in one of Ledieu’s equations, which took the dry bulk density parameter into account.

In order to correct the interpretation of the measured TDR data for base materials, a new model is established, based on limited experimental data. Detailed derivation of this empirical model is described in Chapter 4. Further study is required to obtain a “universal” model for both base and subgrade soils.

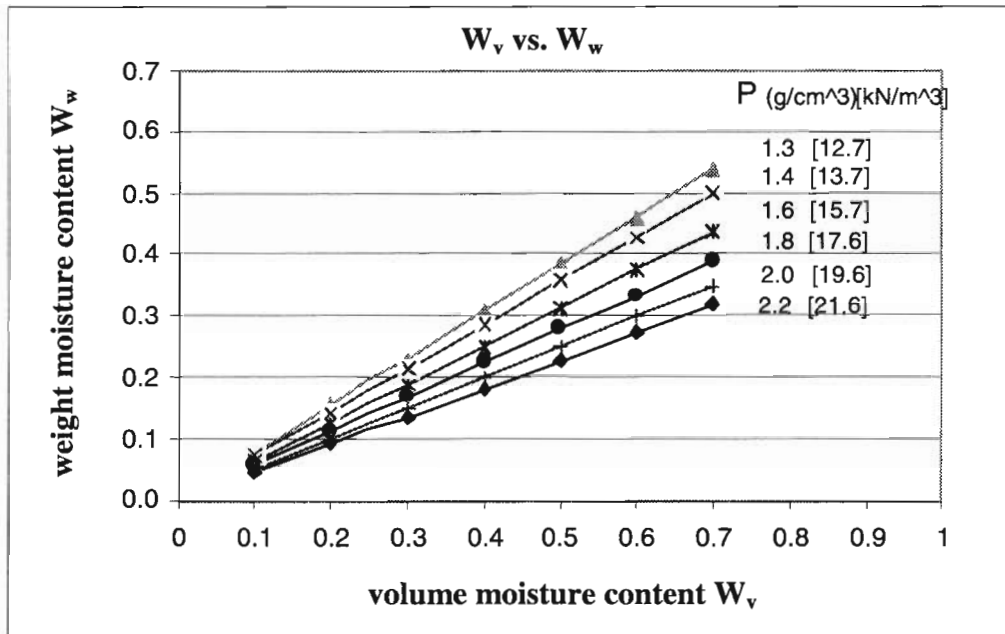


Figure 3.1 Volume and weight moisture contents relation

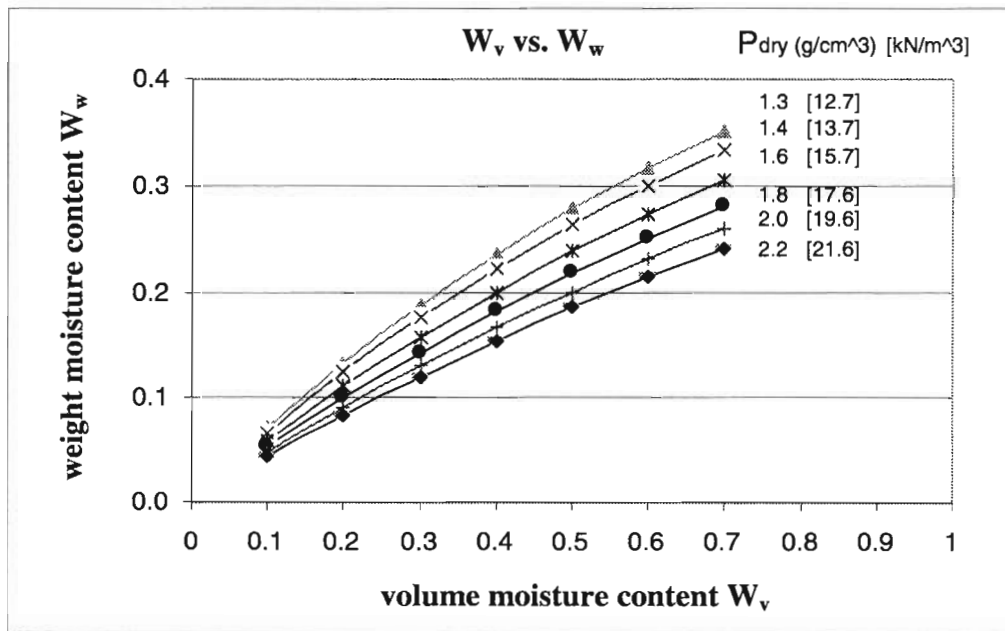


Figure 3.2 Weight and volume moisture contents relation using soil dry density



*Table 3.3 Weight moisture content vs. volume moisture content – measured data*

Weight Moisture Content	Volume Moisture Content		
	No Compaction	Medium Compaction	High Compaction
0.0%	0.066	0.090	0.103
	0.071	0.083	0.106
	0.074	0.086	0.104
	0.067	0.091	0.103
	0.063	0.085	0.102
	0.065	0.086	0.101
3.0%	0.105	0.164	0.192
	0.097	0.157	0.205
	0.097	0.155	0.197
	0.095	0.156	0.185
	0.094	0.155	
	0.098	0.154	
5.0%	0.096	0.202	0.241
	0.082	0.200	0.242
	0.090	0.199	0.230
	0.095	0.192	0.233
	0.101	0.208	0.220
		0.200	0.231
6.46%	0.102	0.324	0.370
	0.111	0.341	0.367
	0.097	0.336	0.354
	0.106	0.342	0.352
	0.103	0.339	0.357
	0.100	0.332	0.365

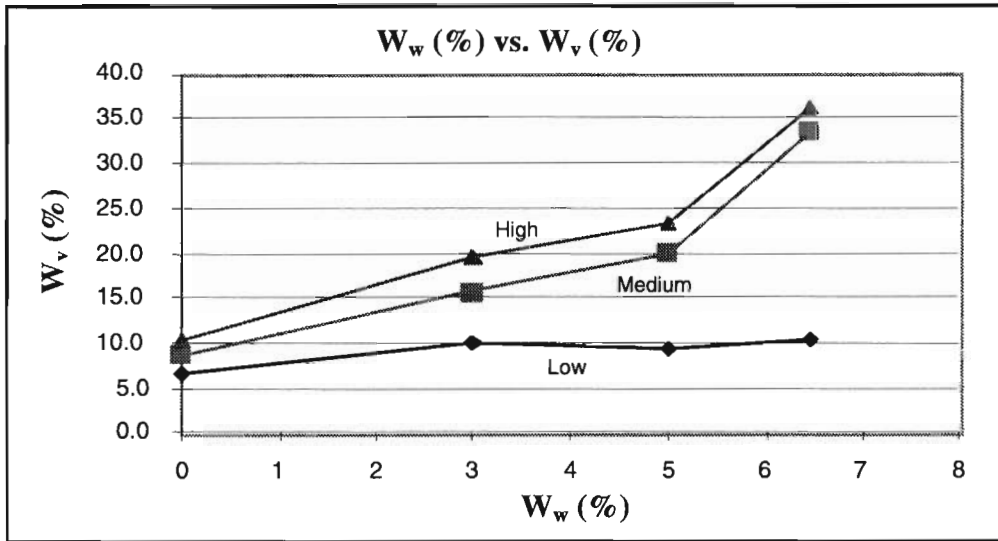


Figure 3.3 Weight moisture content  $W_w$  (%) vs. volume moisture content  $W_v$  (%) under different compactions

Table 3.4 A summary of some existing empirical models [1]

1. Topp et al., 1980	$q = (A+B*Ka +C*Ka^2+D*Ka^3)*10^{-4}$ A = -530, B = 292, C = -5.5, D = 0.043 (4 mineral soils)
2. Ledieu et al., 1986	$q = 0.1138 \text{ SQRT}(Ka) - 0.1758$  $q = 0.1138 \text{ SQRT}(Ka) - 3.38Pb - 0.1529$ (mineral soil) Pb – dry bulk density
3. Maliki & Skierucha, 1989	$q = -19 + \text{SQRT}(388Ka-546.9)/194,$ Ka >= 1.41 (5 mineral)
4. Jacobsen & Schjonning, 1993a	$q = (A+B*Ka +C*Ka^2+D*Ka^3)*10^{-4}$ A = -701, B = 347, C = -11.6, D = 0.18 (10 mineral)



## **CHAPTER 4: FIELD TEST RESULTS OF THE TDR SYSTEM**

### **4.1 TEST SECTION**

The TDR system could be installed into any pavement location. However, for this pilot research project, it was preferable to install the TDRs near an existing weather station and a well-characterized pavement site. Based on the TxMLS test-site document records, the TDR systems were installed approximately 200 ft away from the MLS test pads. The test pads were sections of an in-service pavement located on the southbound and northbound lanes of US281 in Jacksboro, Texas. The southbound and northbound lanes were both fitted with a TDR system. The TDR data would assist the interpretation of the pavement condition under accelerated pavement testing. The main objective of the MLS testing on US281 is to evaluate the effectiveness of two rehabilitation strategies. Hugo et al. [16] documented that different non-destructive tests had been conducted to assist in the site selection, to ensure that test sections had similar characteristics. The data collection included the following:

- 1) Visual inspection of surface distresses (rutting and cracking).
- 2) Structural conditions assessment. Falling Weight Deflectometer (FWD), Seismic Pavement Analyzer (SPA), Spectral Analysis of Surface Waves (SASW), and Ground Penetrating Radar (GPR) were used for this structural assessment.
- 3) Topography survey (the Texas Mobile Load Simulator [TxMLS] requires a nearly flat surface to maintain uniform loads).
- 4) Subsurface condition survey by GPR (underlying cracks, layer thickness, bedrock depth). Non-destructive testing (FWD, SPA, SASW, and GPR) data can render present structural condition.

Two 12-meter sections of pavement with similar material characteristics were selected in the TxMLS study. US281 is a two-lane highway in each direction. In 1994, there was an average use of 3,100 vehicles per day (1550 per direction) of traffic flow. The truck percentage was about 17.4%, and approximately 10% of the total traffic fell on the inside lane. Since the pavement was rehabilitated in 1995, an estimated 9,850 trucks had traveled on the inside lane (or approximately 10,000 to 19,700 ESALs of traffic, depending on the conversion factor used) before the TxMLS was moved onto the test site [17]. The first asphalt layer of the test section was constructed in 1957. Later, there were four major overlays / rehabilitation projects that were completed in 1971, 1976, 1986, and 1995. Figure 4.1 shows the complete pavement history for the southbound and northbound lanes of US281 at the test sections. TxDOT forecasts that the southbound pavement section in the outside lane will be subject to 2 million ESALs over a twenty-year period. The last major rehabilitation was done in 1995 with 50 mm of recycled ACP, using the Remix process. Prior to that, in 1986, there was a major rehabilitation using 85 mm of lightweight aggregate ACP. The inside southbound lane of US 281, Jacksboro, Texas, was closed to traffic in April of 1997 for testing. The TxMLS was then moved onto the test section in May. The outside lane remained open to the public. On the northbound pavement section, the last major rehabilitation was done in 1996,

with 25 mm of new ACP and 25 mm of recycled ACP, known as the “Dustrol” process. Prior to that, in 1986, there was a major rehabilitation using 85 mm of lightweight-aggregate ACP, which was the same as used in the southbound lanes. This lightweight-aggregate layer, 25 mm was recycled in the Dustrol process.

Nuclear Density Gauge (NDG) tests were conducted to measure the in-situ ACP density. The average density for the southbound lane, which contains a significant amount of lightweight aggregate in the ACP layers, was 1875 kg/m<sup>3</sup> (117 pcf). For the base and subgrade, the typical soil dry density is about 2000 kg/m<sup>3</sup> (125 pcf) and 1750 kg/m<sup>3</sup> (109 pcf), respectively [17]. For the top 50 mm remixed layer, approximately 12-13% of air void was found in the non-trafficked area and 5.4% under the trafficked area. The GPR data and construction records indicated that the bedrock is very shallow at the test section. The depths of the bedrock were found to be 2.69 m and 2.54 m for the left and right wheel paths, respectively, by using an extended Dynamic Cone Penetrometer (DCP).

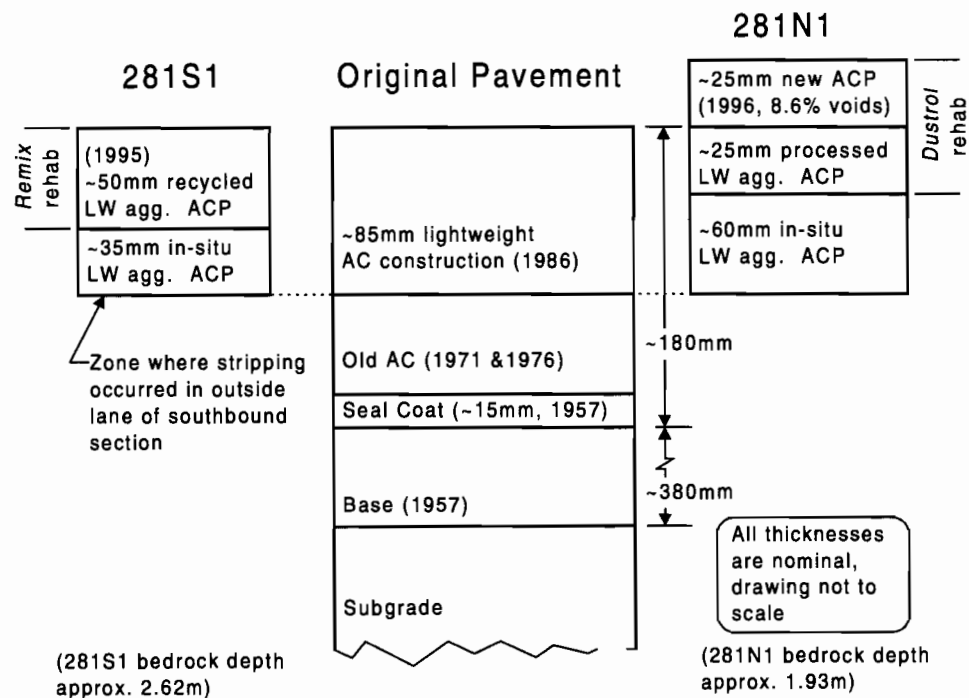


Figure 4.1 Pavement sections of southbound and northbound US281

## 4.2 TEMPERATURE VARIATION AND SUBSURFACE MOISTURE MOVEMENT

Temperature sensors were installed at three different depths, which were 12.7 mm, 88.9 mm, and 165.1 mm from the surface of the ACP layer. Pavement temperature data were collected both inside and outside the TxMLS to determine the temperature variation. On

a typical sunny day, the most variation occurred at a depth of 12.7 mm, which was typically 17 °C hotter outside than inside the TxMLS at noon. At a depth of 88.9 mm, a 7 °C difference was observed. For overcast/rainy days, less than 2 °C difference was observed at all three depths. As expected, higher temperature variations occurred outside than inside the MLS. At a depth of 12.7 mm, daily temperature variations (high minus low) of 11 °C and 28 °C were found inside and outside the TxMLS, respectively (Figure 4.2). At the 88.9 mm depth, the temperature variation decreased. The effect of shade, whether from the TxMLS cover or clouds, greatly decreased the range of pavement temperature. Shade also tended to increase the lag time between maximum air temperature and maximum pavement temperature. The pavement temperature outside the TxMLS at a depth of 12.7 mm experienced almost no time lag on a sunny day. However, at the same depth, it took 3 hours for the pavement inside the MLS to respond to an increase in sunshine.

The cover provided by the TxMLS consistently reduces the daily temperature swing by 50%. Without the TxMLS cover, the daytime highs were higher (due to sunlight) and the nighttime lows were lower (no wind protection). This tendency is most noticeable at the top 12.7 mm of ACP, and it holds throughout the summer and winter months. A depth of 165 mm of ACP plus MLS cover makes the day/night temperature change insignificant.

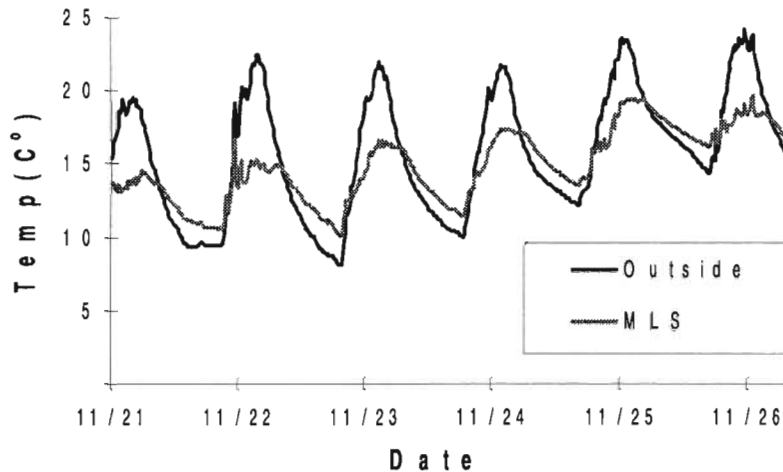


Figure 4.2 Temperature variations at a depth of 88.9 mm

### 4.3 TDR INSTALLATION PROFILE

The soil moisture content can be determined by measurement of the dielectric constant  $\epsilon$  of the soil, because the dielectric constant  $\epsilon$  of free water is at least 15 times greater than that of common soil constituents. The dielectric constant  $\epsilon$  is measured using a Time Domain Reflectometer (TDR). Eight TDRs were embedded in the base and subgrade, as shown in Figure 4.3. There were 3 holes to accommodate these 8 TDR probes. Two of the holes had 3 TDR probes, and the third one had 2 TDR probes. The 2

holes having 3 TDR probes were located in the center of each wheel path. The third hole was located in the unpaved shoulder. After the TDR probes were installed, the holes were first back-filled with the original materials of subgrade and base, then with a cold-mix AC to replace the ACP. TDR readings located in the unpaved shoulder were used as references because they were very sensitive to rainfall events.

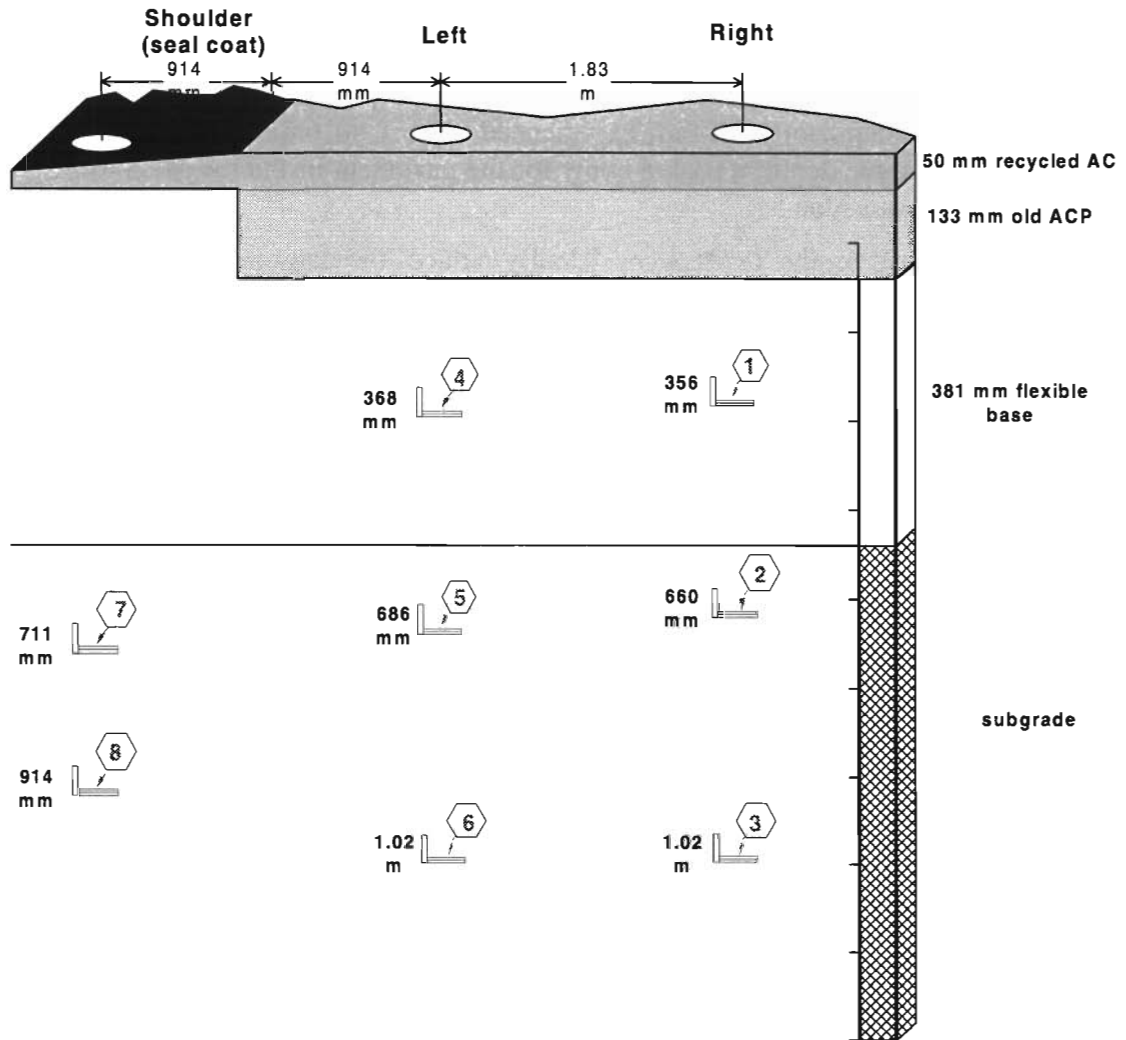


Figure 4.3 Southbound US281, TDR sensor installation profile

#### 4.4 TDR INTERPRETATION METHODS AND TEST RESULTS

The TDR probes were installed at both the southbound and northbound sites of US281, Jacksboro, Texas. The first testing was done at the southbound site. The TDR probes could not be moved because they were non-reusable. TxDOT began to get regular field data in September 1997 from the southbound site, and in August 1998 from the northbound site.

#### 4.4.1 Interpretation Method for Base Layer

The TDR readings represent the volume moisture content  $W_v$  of the surrounding soil. A very notable discovery from this study is that the volume moisture content  $W_v$  of the base materials/soils was very sensitive to compaction conditions, while the weight moisture content  $W_w$  was not (see Table 3.2 & Figure 3.3). This phenomenon is easy to explain by considering the definitions of weight moisture content  $W_w$  and volume moisture content  $W_v$ .  $W_w$  is independent of the total volume of the soil, while  $W_v$  is a function of soil density, which is a function of the total volume of the soil. The experimental data indicated that for the base layer, the volume moisture content  $W_v$  was not a simple function of the dielectric constant  $\epsilon$  of the material, but a complex function of dielectric constant  $\epsilon$  and compact effort  $p$ . This compact effort  $p$  was related to the density of the soil. The compaction changed the structure of the soil particles, which in turn changed the relationship between weight moisture content  $W_w$  and volume moisture content  $W_v$ . Further study is needed to give a quantitative correlation among  $W_w$ ,  $W_v$ , and  $p$ . Based on this fact, an interpretation model for the compacted base materials was directly established to relate the weight moisture content  $W_w$  and dielectric constant  $\epsilon$ . Unlike  $W_v$ ,  $W_w$  does not depend on compact effort  $p$ , but primarily on a simple function in terms of dielectric constant  $\epsilon$  of the material. The TDR reading can be restored back to the dielectric constant  $\epsilon$  by reversing the Ledieu equation (the Ledieu equation is expressed as Eq. (3.5)):

$$\epsilon = ((W_v + 0.1758)/0.1138)^2 \quad (4.1)$$

The compact condition of the base materials was found to be similar to the high compaction level in Table 3.2. An empirical equation is derived from those experimental data in Table 3.2 as follows:

$$W_w(\%) = (0.0506 * \ln(\epsilon) - 0.088) * 100 \quad (4.2)$$

The accuracy of equation (Eq. (4.2)) can be improved if more compaction data as in Table 3.2 are available, especially for higher weight moisture content  $W_w$ , because many of the field data fall into this range.

#### 4.4.2 Interpretation Methods for Subgrade

There are several existing empirical models to calculate the volume moisture content  $W_v$  of the subgrade by knowing dielectric constant  $\epsilon$  of the subgrade soils. Ledieu's model (1986) and Topp's model (1980) are two of the best established empirical models which convert the dielectric constant  $\epsilon$  into volume moisture content  $W_v$  with a sufficient precision for engineering applications. Ledieu's method is the default method for the TDR system developed in this study, which is expressed in Eq. (3.5), and Topp's method is expressed in Eq. (4.3):

$$W_v = (-530 + 292 * \epsilon - 5.5 * \epsilon^2 + 0.043 * \epsilon^3) * E(-4) \quad (4.3)$$

Based on the relationship among  $W_w$  and  $W_v$  and  $\rho_{dry}$ , as established in Equations (3.7) and (3.9),  $W_w$  can be obtained when  $W_v$  and  $\rho_{dry}$  are given. The predicted results using these two models are summarized in Tables 4.3 and 4.4.



### 4.4.3 Field Test Results

There are eight TDR probes at each test site. Four TDR probes are selected to represent the measurement of the moisture content of the base materials (#4), the subgrade at right (#3), left (#5), and shoulder (#8) positions, for the southbound test site, as in Figure 4.3. Five TDR probes are selected to represent the base materials at the right (#1), left (#4), and shoulder (#7) positions, and the subgrade at the right (#3) and left (#6) positions, for the northbound test site.

The converted  $W_w$  data (at the southbound test site) are shown in Figures 4.4 to 4.7. All original data come from the TDR field readings through the on-site weather station. There was no data collection between November 12<sup>th</sup> and November 20<sup>th</sup>, which explains the broken areas in some plots. Some out-of-range data were eliminated from these figures. Criteria for this pre-selection (elimination) were: if the TDR reading ( $W_v$ ) is less than 0.15 or greater than 0.60, or the variation of the consecutive data varies more than 33%, then those data were not selected, because they were not reliable; thus they had to be eliminated. The precipitation is also plotted onto the same figure, with another Y axis, to show the cause of the variation in TDR readings. In the  $W_w$  conversion, the value of  $\rho_{dry}$  for the base and subgrade are 2000 kg/m<sup>3</sup> and 1750 kg/m<sup>3</sup>, respectively. This value is based on true field data from the southbound test site. Table 4.1 covers the overall quality evaluation based on 8 TDRs' readings at the southbound test site from September 1997 to March 1998. Table 4.2 covers the overall quality evaluation based on 8 TDRs' readings at the northbound test site from August 1998 to November 1998. In Tables 4.1 and 4.2, a "good" rating means that the moisture content variation corresponds to the precipitation variation, and only a small amount of data was eliminated for being out of range. An "ok" means that the moisture content variation corresponds to the precipitation; however, a relatively high amount of data was eliminated for being out of range. A "/" means that the specific TDR probe may have encountered some problems, since during those months the data did not change at all with the precipitation. Tables 4.3 and 4.4 describe the monthly average of weight moisture contents  $W_w$  for the selected TDR probes.

At the southbound test site, the weight moisture content  $W_w$  at the base layer was measured by TDR #4. The overall average  $W_w$  calculated from Eq. (3.2) is 5.53%, as shown in Tables 4.3 and 4.4, and shows only a minor discrepancy of about 0.4% with the true field measurement of 5.3%;  $W_w$  at the subgrade layer was measured by TDRs #3, #5, and #8. The overall average  $W_w$  calculated from the Ledieu (Topp) methods were 15.57 (15.70)%, which are good enough when compared with the typical real field measurement of 16.6% (the error is about 5%).

At the northbound test site, the weight moisture content  $W_w$  at the base layer was measured by TDRs #1, #4, and #7. The overall average  $W_w$  calculated from Eq. (4.2) is 8.18% (as shown in Tables 4.3 and 4.4);  $W_w$  at the subgrade layer was measured by TDRs #3, and #6. The overall average  $W_w$  calculated from the Ledieu (Topp) methods are 21.22 (20.78)%. There are no real field measurements for comparison at the

northbound test site. The dry density  $\rho_{dry}$  used to convert  $W_v$  to  $W_w$  was based on the southbound measured data. The ranges of  $W_v$  from the northbound side are reasonable.

As shown in Figures 4.4 to 4.7, the researchers found that the variations in the TDRs' data corresponded well with changes in the rainfall data, as expected. The monthly average and the overall average of weight moisture content  $W_w$  (%) are reliable.

*Table 4.1 The overall evaluation of the 8 TDRs at southbound US281 test site*

Month	#1 (base)	#2	#3	#4 (base)	#5	#6	#7	#8
Feb.	ok	good	good	good	good	ok	good	good
Jan.	good	good	good	good	good	good	good	good
Nov	good	good	good	good	good	good	good	good
Oct.	good	ok	good	good	good	ok	good	good
Sept.	good	ok	good	good	good	ok	good	good

*(Note: TDRs #2, #3, and #5-#8 were in subgrade)*

*Table 4.2 The overall evaluation of the 8 TDRs at northbound US281 test site*

Month	#1 (base)	#2 (base)	#3	#4 (base)	#5 (base)	#6	#7 (base)	#8
Nov.		good	good	good	good		good	
Oct.	good	good	good	ok	good	good	ok	ok
Sept.	good	good	good	good	ok	ok	ok	good
Aug.		ok	ok	ok	good	ok	ok	good

*(Note: TDRs #3, #6, and #8 were in subgrade)*

*Table 4.3 TDRs monthly average  $W_w$  (%) for southbound US281 test site*

Month	TDR	#3 (subgrade)	#4 (base)	#5 (subgrade)	#8 (subgrade)
Feb.		14.77 (15.25)	5.68	17.41 (17.44)	15.96 (16.4)
Jan.		15.5 (15.98)	5.91	17.22 (17.54)	17.11 (17.46)
Nov.		13.9 (14.36)	5.18	15.9 (16.31)	14.32 (15.78)
Oct.		14.25 (14.71)	5.38	16.35 (16.72)	15.12 (15.57)
Sept.		14.12 (14.6)	5.49	16.7 (17.09)	14.92 (15.4)
	<b>Average</b>	<b>14.51 (14.98)</b>	<b>5.53</b>	<b>16.72 (17.08)</b>	<b>15.49 (15.92)</b>

*(base—experimental method in this study; subgrade—Ledieu (Topp) method)*

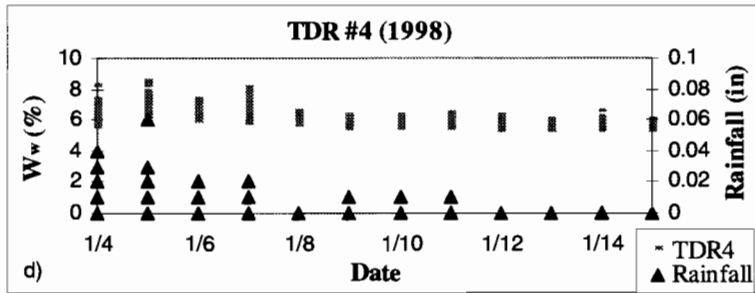
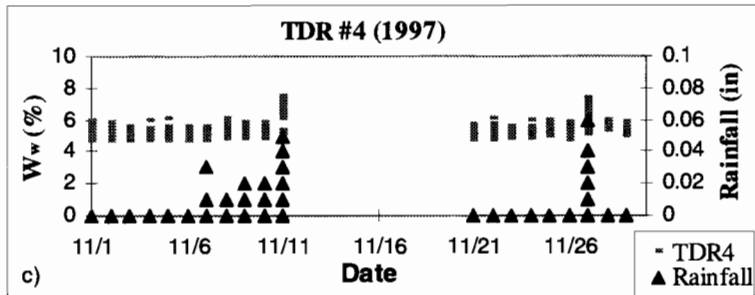
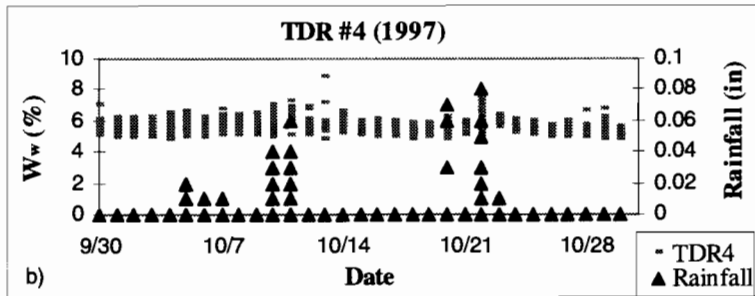
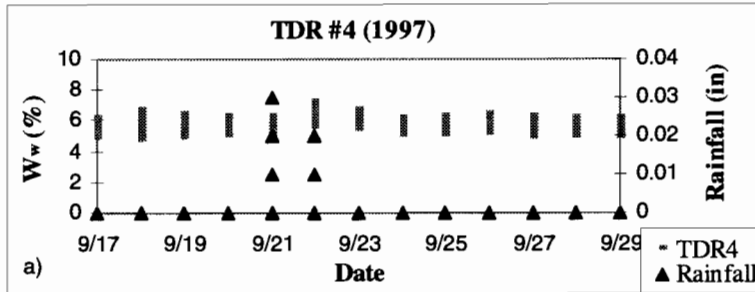
**overall average: base—5.53 %; subgrade—15.57 ( 15.70) %**

*Table 4.4 TDRs monthly average  $W_w$  (%) for northbound US281 test site*

Month \ TDR	#1 (base)	#3 (subgrade)	#4 (base)	#6 (subgrade)	#7 (base)
Nov. 98	8.12	20.3 (20.08)	6.77	21.29 (20.86)	9.02
Oct. 98	8.63	20.8 (20.5)	7.71	21.69 (21.12)	9.09
Sept. 98	8.75	21.43 (20.98)	7.75	22.04 (21.36)	9.05
Aug. 98		20.5 (20.26)	6.99		7.81
<b>Average</b>	<b>8.50</b>	<b>20.76 (20.46)</b>	<b>7.31</b>	<b>21.67 (21.11)</b>	<b>8.74</b>

*(base—experimental method in this study; subgrade—Ledieu (Topp) method )*

**overall average: base—8.18 %; subgrade—21.22 (20.79) %**



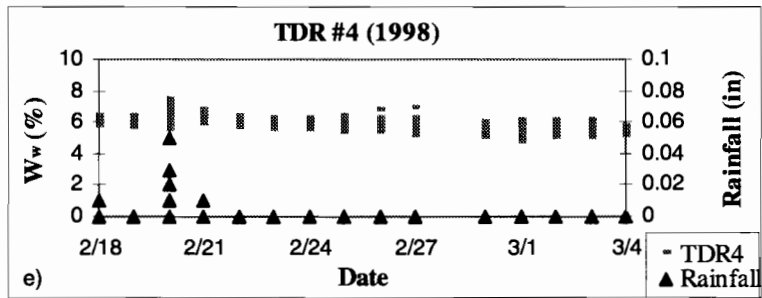
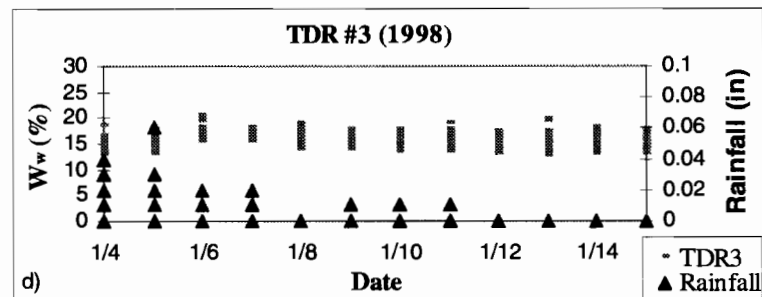
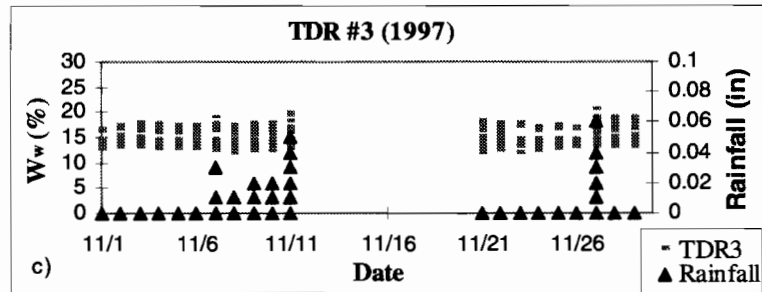
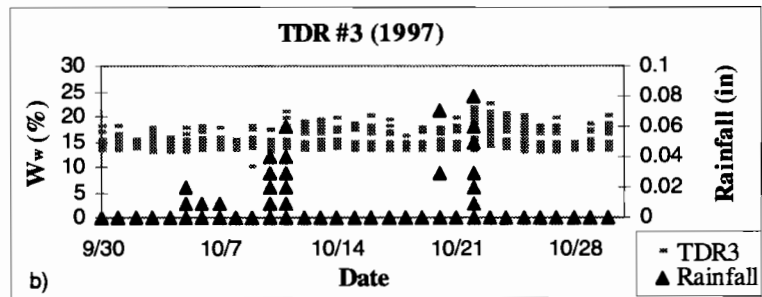
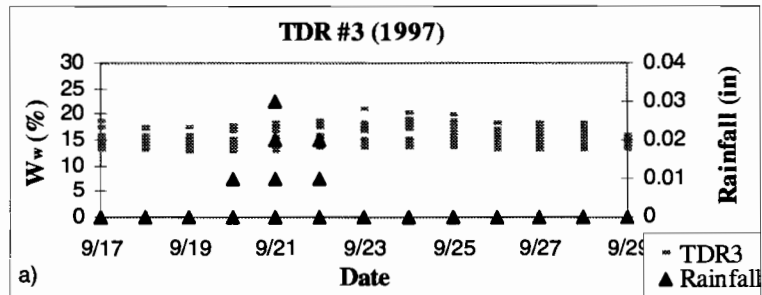


Figure 4.4 Rainfall and  $W_w$  for southbound TDR #4 in the base layer (0.368 m)



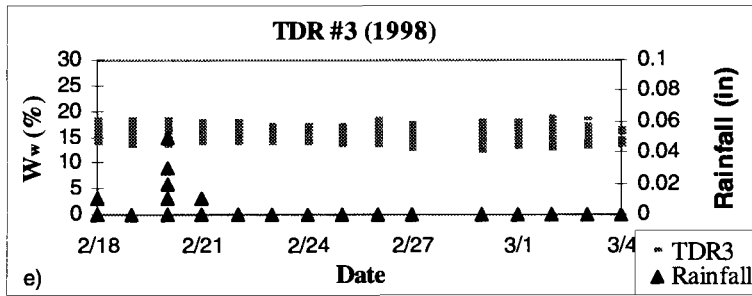
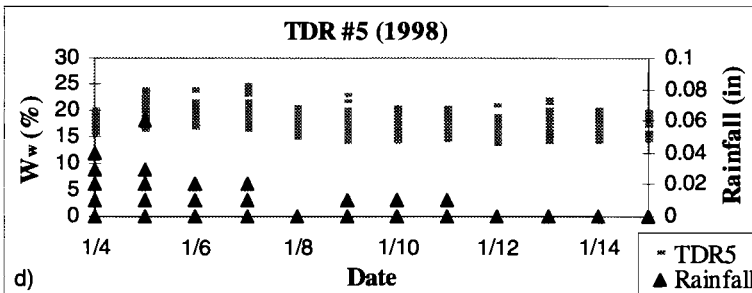
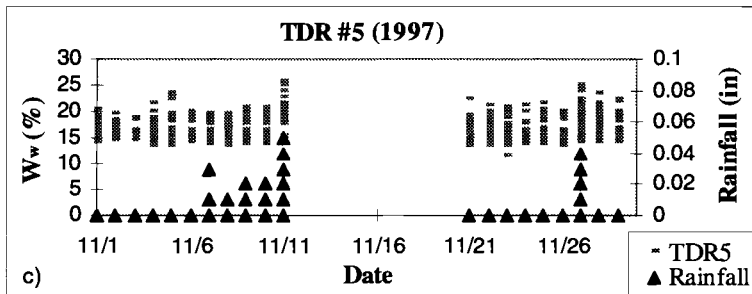
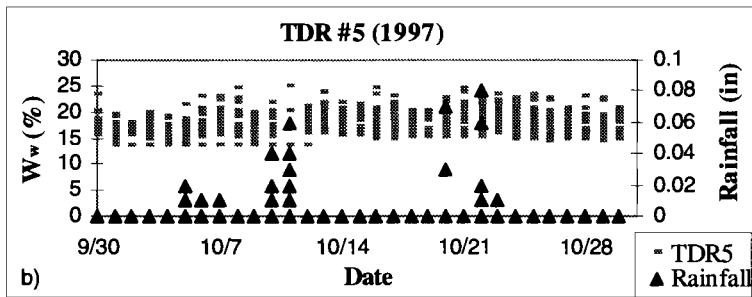
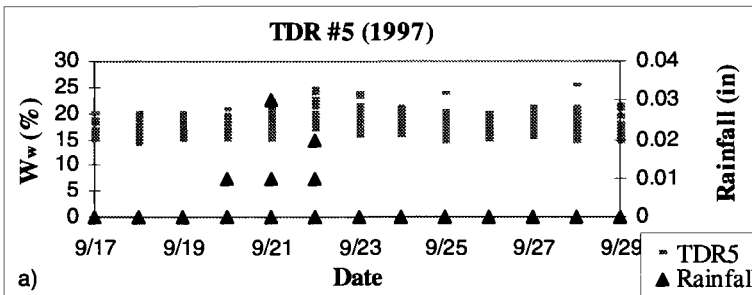


Figure 4.5 Rainfall and  $W_w$  for southbound TDR #3 in the subgrade layer (1.02 m)





## **CHAPTER 5:**

### **GPR SYSTEM: IMPLEMENTATION AND TEST RESULTS**

#### **5.1 BACKGROUND OF GPR TECHNIQUE**

The Ground Penetrating Radar (GPR) technique is another technique which uses electrical properties to measure the in-situ soil moisture content.

The GPR operates by transmitting short pulses of electromagnetic energy into the pavement [18]. When encountering dielectric discontinuities in the subsurface, part of the transmitted waves are reflected and picked up by the receiver, and the received signal is then amplified and analyzed. The propagation of the electromagnetic waves in the ground depends on the electrical properties of the media. The two most important factors affecting the propagation of radar pulses in any media are the dielectric content  $\epsilon$  and the electrical conductivity  $\sigma$ . According to different needs for depth and spatial resolution measurements, different kinds of GPR systems can be chosen. The operating frequencies are from 10 MHz to 2 GHz for moisture content measurement. A typical GPR system is shown in Figure 5.1

For adequately high frequencies, the relationship between the dielectric constant  $\epsilon$  and the volume moisture content  $W_v$  of the soil is expressed in Eq. (3.5). There are several methods to calculate the dielectric constant  $\epsilon$  by GPR. The inversion method is used in this study to convert the reflected signal to the material's dielectric constant.

##### **5.1.1 Inversion Method**

The inversion method applies the time domain Transmission Line Matrix (TLM) method [19-22] and the layer stripping technique to invert the pre-processed GPR voltages to the dielectric constant data of each layer [23-27]. Because both the depth and spatial resolutions are needed for pavement moisture measurement, the traditional GPR data processing method can not produce an accurate result. In this study, the time domain TLM method with layer stripping technique is applied for moisture content determination.

The TLM method is a time-domain numerical method solving Maxwell's equations by using a transmission line analogy. The observed space is divided into small cells and a transmission line network is used in each cell to characterize the cell's electromagnetic performance. The electrical and magnetic fields are simulated by voltages and currents in the transmission line network. For a given transmitted waveform, the received signal can be constructed by using this method, and consequently the dielectric images of each layer are reconstructed. Since TLM simulation must be conducted in a finite space, a Perfect Matched Layer (PML) [23-24] is placed at the boundaries (where the simulation space ends) to simulate infinite boundaries.

The one-dimensional layer stripping method is used to reconstruct the 1-D dielectric constant profile (with respect to depth) in the pavement. Consider the N-Layer information profile shown in Figure 5.2. The background profile function for the first



layer is P(1) with a homogeneous distribution of both the dielectric constant and conductivity. For the (i)<sup>th</sup> layer, the background profile function is P(i) with an (i)<sup>th</sup> layer reconstructed. The information from previously-inverted layers are used, and the rest of the layers are considered to have the same values with that of (i-1)<sup>th</sup> layer. The received signal  $y_{p(i-1)}(t)$  due to the profile P(i-1) contains only the reflection from the first layer to the (i-1)<sup>th</sup> layer. The difference between  $y_{p(i-1)}(t)$  and the  $y_{p(i)}(t)$  due to (i)<sup>th</sup> profile P(i) will be zero from  $t = 0$  to  $t = t_i$ , which corresponds to the (i)<sup>th</sup> interface.

The rising edge of  $y_{p(i)}(t) - y_{p(i-1)}(t)$  marks the starting time of the reflection of the (i)<sup>th</sup> boundary, which is determined as a certain percentage of the peak, due to noise and the non-linearity of space and time in a dispersive medium. In this program, 3% is used as the upper limit to control the iterations for the required accuracy. Three groups of data are needed in this program: measured data, data computed from an assumed profile and data from a background profile. The received signals from these profiles are called  $y_{real}(t)$ ,  $y_{assume}(t)$  and  $y_{back}(t)$ , respectively. By calculation, the real reflection coefficient is calculated as:

$$\Gamma_{real} = \frac{y_{real}(t_i) - y_{back}(t_i)}{y_{assume}(t_i) - y_{back}(t_i)} [\Gamma_{assume}(i) - \Gamma_{back}(i)] + \Gamma_{back}(i) \quad (5.1)$$

And then the (i)<sup>th</sup> layer's dielectric constant  $\epsilon$  can be calculated as:

$$\epsilon_{ri} = \frac{1}{2(\Gamma_{real}(i) + 1)} - \frac{\sigma_i \Delta x \eta_0}{2\sqrt{2}} \quad (5.2)$$

Where  $\sigma_i$  is the conductivity of (i)<sup>th</sup> layer.  $\Delta x$  is the grid size and

$$\eta_0 = \sqrt{\mu_0 / \epsilon_0} \quad (5.3)$$

Where  $\mu_0$  is the magnetic permeability of vacuum, and  $\epsilon_0$  is the dielectric constant of vacuum.

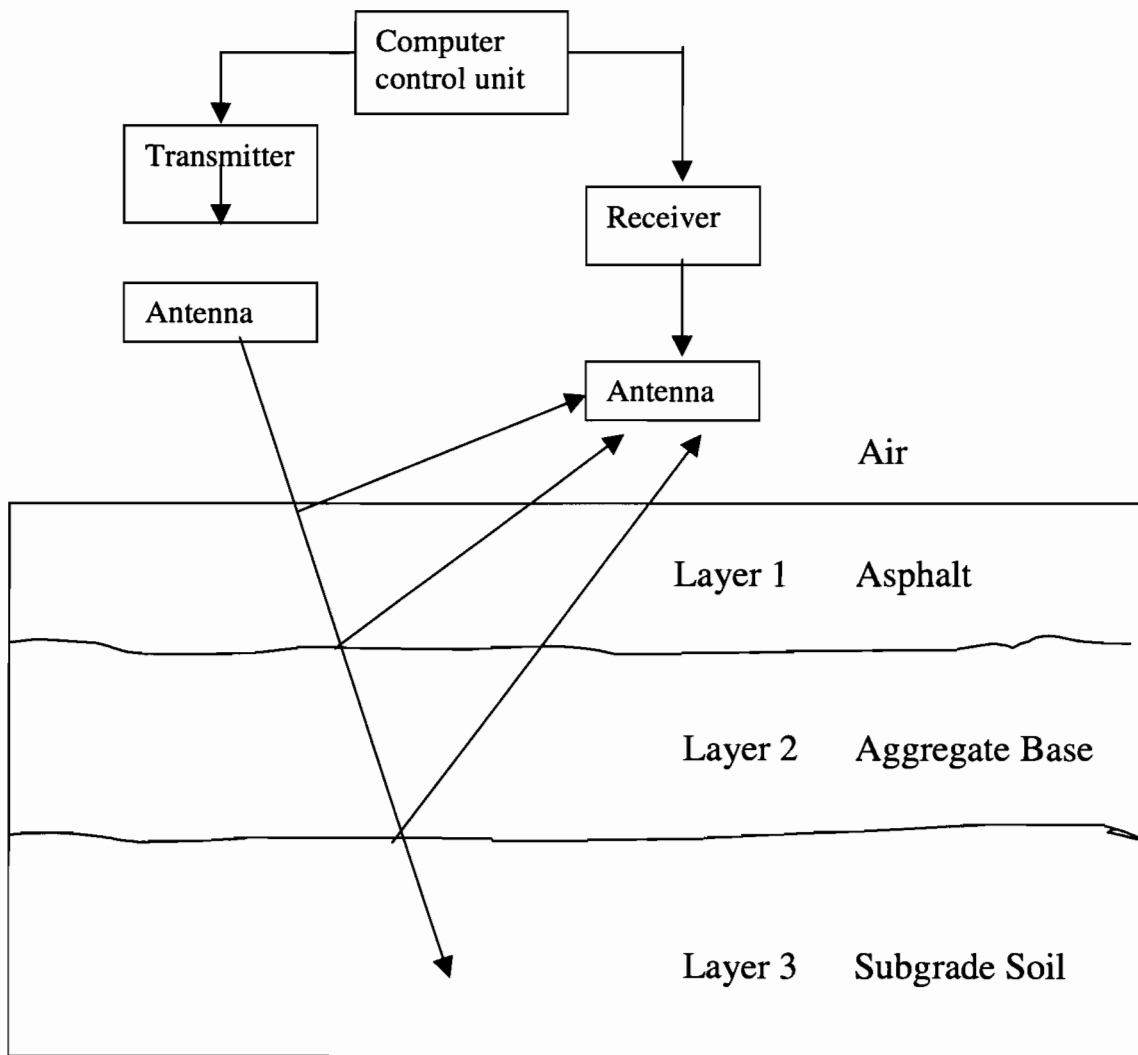


Figure 5.1 A block diagram of a GPR system used in the moisture content measurement

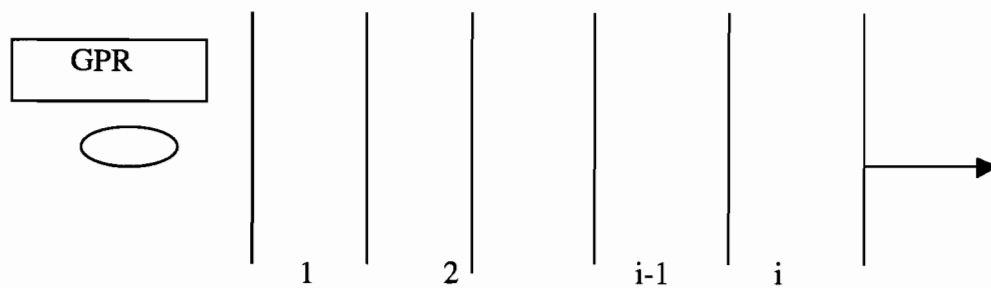


Figure 5.2 An N-Layer information profile (left (top) → right (bottom))

## **5.2 COMPONENTS OF GPR SYSTEM**

A GPR system [28-33] consists of three major parts: a transmitter, a receiver and a computer control unit.

### **Transmitter**

The transmitter sends out a series of short pulses of high electromagnetic energy into the ground. The propagation of the electromagnetic waves in the ground depends on the electrical properties of the ground.

### **Receiver**

The receiver picks up wave information of all the pavement layers.

### **Computer Control Unit**

The computer control unit stores, processes, and controls the testing program.

## **5.3 GPR SYSTEM TEST SET-UP**

The GPR system employed for this project is called the EKKO1000 GPR system, and was developed by Sensor & Software Corp. The reason for choosing the EKKO1000 GPR system is because it can provide both the depth and spatial resolutions for this study. The basic specifications are listed as follows:

Frequency: 1.2 GHz

Time window: 20 ns

Sampling rate: 100 ps

Pulse Voltage: 200 V

### **5.3.1 Laboratory Test Set-Up**

Before field measurements were performed, the laboratory verification for the effectiveness of this GPR system was conducted with sand as the sample. The first experiment used a case of sand, and the moisture content increased from 0 to 4.76%; 9.1%; 13.04%; and 16.7%, in that order. The second experiment used the same amount of sand consisting of two layers of different moisture content. The moisture content of layer 1 increased from 0 to 4.76% then 9.1%, while the moisture content of layer 2 was kept at 13.04%. The configuration of the experiments is shown in Figure 5.3.

The sand parameters are:

Density of the sand:  $\rho_{\text{dry}} = 1.62 \text{ g/cm}^3$

Experiment1 (one layer): thickness of the sand layer: 175 mm

Experiment2 (two layers): thickness of the sand layer 1: 125 mm, and  
thickness of the sand layer 2: 125 mm

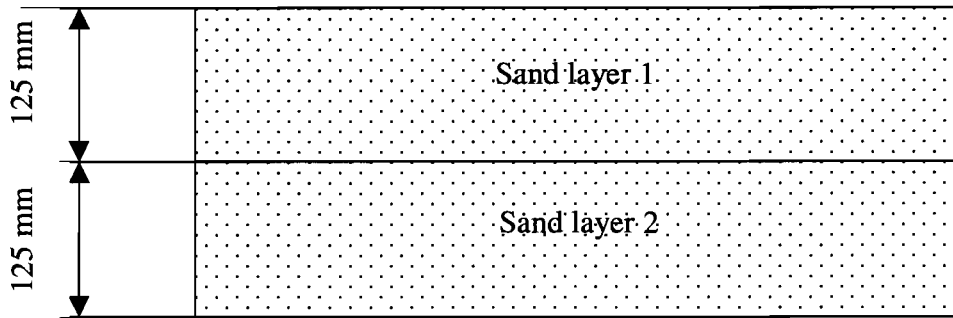


Figure 5.3 Sand box with two layers of sand at different moisture contents

### 5.3.2 Field Test Set-Up

The field data were collected from 4 layers of the southbound US281, TxMLS test site in Jacksboro, Texas. Table 5.1 gives the approximate layer thickness and dielectric constant of those layers.

*Table 5.1 Background knowledge for southbound US281, Jacksboro, Texas.*

Number of layer	Name of layer	Thickness (mm)	Dielectric Constant $\epsilon$
Layer 1	Asphalt	175~200	3~6
Layer 2	Aggregate base	380	4~8
Layer 3	Subgrade soil	200~300	10~30
Layer 4	Bedrock		

## 5.4 GPR DATA PROCESSING

### 5.4.1 Basic Procedure

The basic GPR data processing procedure for measurement of highway pavement moisture content is briefly introduced in this section. Generally, there are four steps for processing GPR data. Step 1: edit and compile the initial data. Step 2: apply a time gain and filtering technique according to the required processing. Step 3: translate the data that are in the GPR format to a text format so that further processing can be performed. Step 4: analyze the pre-processed data and obtain the final result. Usually the first three steps are accomplished by the GPR system when the measurement is finished. We can then decide which kind of filter to apply and what stack sizes are needed, depending on the practical conditions in the presence of noise and distortion.

### 5.4.2 Inversion Results of Synthetic Data

The inversion method developed in this study investigated several synthetic inversion cases. Synthetic data were obtained by using forward modeling upon the assumed layer distributions, then the inversion process was performed, layer by layer, to calculate the dielectric constant of each assumed layer.

The transmitted wave being used is a half-wave sine-squared function with a pulse width of 1 ns. The formation consisted of 12 layers where each layer is 10 cm thick, with a 1 cm grid size. Figure 5.4 shows an application of dielectric constant reconstruction. We can see that the dielectric constant is recovered satisfactorily for all 12 layers.

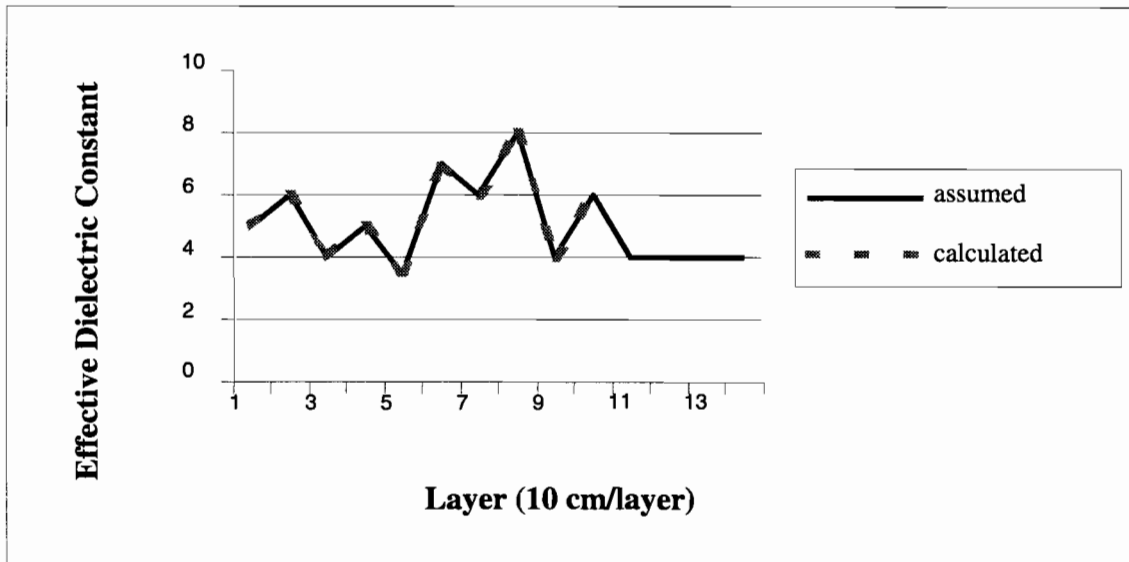


Figure 5.4 Inversion result using synthetic data

### 5.4.3 Inversion Results of Field Data

The field testing data and their background parameters are described in Section 5.1.1. Using the inversion technique described in the previous section, the dielectric constant of the subsurface layers can be acquired. There are some differences between the parameters set up for the synthetic inversion and the practical inversion. The transmitted pulse, also called the direct wave, is generated by setting antennas in the air. The frequency is 1.2 GHz and a 1 mm grid size is chosen to achieve a higher resolution and eliminate the influence of quantization noise. Tables 5.2 and 5.3 are the inverted results using GPR data measured at the northbound side of US281, Jacksboro, Texas, on October 19, 1998. In both cases the same antenna height of 27.5 cm from the pavement surface was selected. The only difference in Tables 5.2 and 5.3 is the sampling rate, and a higher sampling rate gives more accurate results.

*Table 5.2 Inversion results when sampling rate is 50 ps*

Number of layer	Name of layer	Thickness (mm)	Dielectric Constant	$W_w$ (Moisture Content %)
1 <sup>st</sup> layer	Asphalt	160	2.67	0.6
2 <sup>nd</sup> layer	Aggregate base	310	3.3	2.1
3 <sup>rd</sup> layer	Subgrade soil		12.8	12.83
4 <sup>th</sup> layer	Bedrock			

*Table 5.3 Inversion results when sampling rate is 100 ps*

Number of layer	Name of layer	Thickness (mm)	Dielectric Constant	$W_w$ (Moisture Content %)
1 <sup>st</sup> layer	Asphalt	195	2.8	1.1
2 <sup>nd</sup> layer	Aggregate base	395	4.1	3.5
3 <sup>rd</sup> layer	Subgrade soil	460	13.6	15.03
4 <sup>th</sup> layer	Bedrock			

The above test results were close to the expected values. However, the results were influenced by background noise, especially those weak signals reflected from deeper layers under ground. Thus, the determination of moisture content of pavement layers using the GPR test was not reliable due to the rather long waveform tail and the unclear received signal.

## 5.5 TEST RESULTS

### 5.5.1 Laboratory Test Results

Figure 5.5 describes the trace received directly by the receiver in the air, and only the direct transmitted wave is shown. Figure 5.6 describes one of the traces extracted from the profile measured from the two-layer sand sample.

Tables 5.4 and 5.5 compare the real moisture content to the GPR-measured values using the one-layer and two-layer samples. The direct GPR reading consisted of the volume moisture content  $W_v$ . The weight moisture content  $W_w$  is converted by Eq. (3.5) (Ledieu's Equation). The converted weight moisture contents  $W_w$  of the sand, under laboratory conditions, are acceptable. The maximum discrepancy, located in the second layer, is slightly less than 4%. For the one-layer sand and the first layer of the two-layer sand, the GPR-measured moisture content results matched the real value very well, and the maximum discrepancy is less than 1%. As mentioned before, the

current GPR test results are not satisfactory and reliable, and a more effort is being put forth.

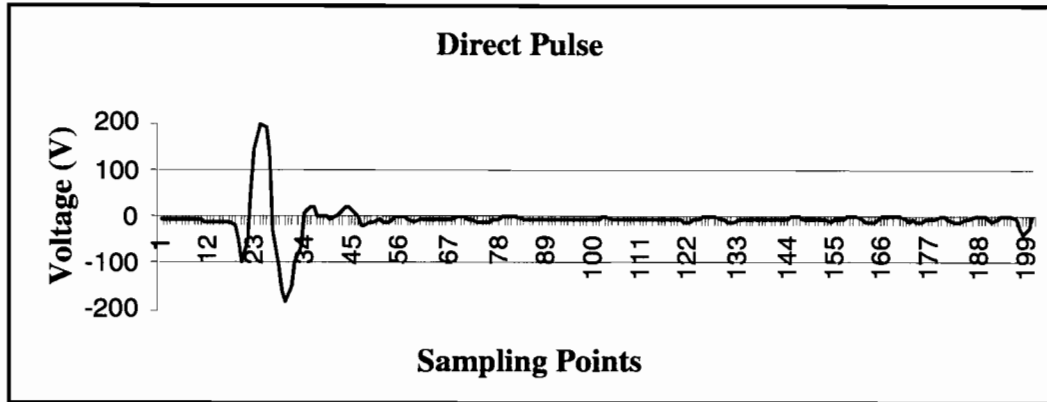


Figure 5.5 Waveform of the direct wave

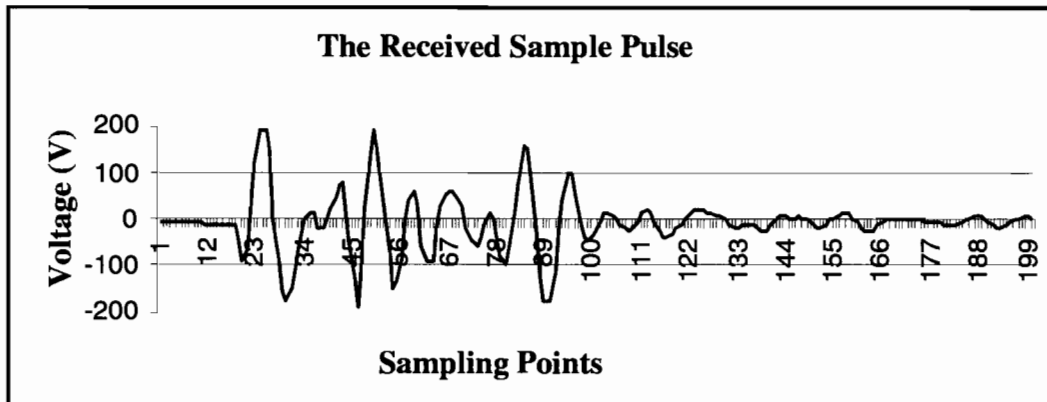


Figure 5.6 A trace from the two-layer sand sample

### 5.5.2 Field Test Results

During the field measurements, the frequency was set to 1.2 GHz; and the time window was selected at 50 ns to cover the required penetration depth. The height of the antennas was set at 0 cm and 27.5 cm from the surface of the pavement, and sampling intervals were set at 10 ps, 50 ps and 100 ps, respectively. Six groups of field data were collected. However, the quality of the field data was not satisfactory due to the tail of the direct wave (which was rather long) and thus resulted in low quality of the received signal. A further study is required to improve the clarity of the waveform under field conditions.

*Table 5.4 Comparison of the one-layer sand real moisture content and the GPR result*

Measured dielectric constant $\epsilon_i$	$W_v$ -measured (volume moisture content by GPR) (%)	$W_w$ -calculated (weight moisture content by Ledieu's) (%)	$W_w$ -real (%)	$(W_w$ -real) – $(W_w$ -calculated) (%)
2.77	1.36	0.08	0.0	0.08
4.46	6.45	3.83	4.76	0.93
9.11	16.76	9.38	9.1	-0.28
13.2	23.8	12.8	13.04	0.24
19.5	32.7	16.8	16.7	-0.1

*Table 5.5 Comparison of the two-layer sand real moisture content and the GPR result*

Measured dielectric constant $\epsilon_i$	$W_v$ -measured (volume moisture content by GPR) (%)	$W_w$ -calculated (weight moisture content by Ledieu's) (%)	$W_w$ -real (%)	$(W_w$ -real) – $(W_w$ -calculated) (%)
1 <sup>st</sup> layer				
2.77	1.36	0.08	0.0	0.08
4.46	6.45	3.83	4.76	0.93
9.11	16.76	9.38	9.1	-0.28
2 <sup>nd</sup> layer				
13.17	23.5	16.6	13.04	-3.56





## CHAPTER 6: CONCLUSIONS

The conclusions are given as follows:

### 6.1 TDR SYSTEM

In this research, the pre-purchased TDR system to measure soil moisture content has been successfully modified. A datalogger with Programmable Read-Only-Memory (PROM) has been added into the Tektronix 1502B TDR cable tester, which enables the TDR system to automatically control the sequence of the data acquisition and measurement. The temperature sensors installed in the weather station also performed well. This modified TDR moisture content measurement system has satisfactory accuracy in both the laboratory and field environments. The TxDOT two-year field test results indicated that the following conclusions could be drawn based on this improved TDR system:

- 1) Evaluation indicated that some existing models (such as Ledieu et al. 1986, Topp et al. 1980) to predict the moisture content from the dielectric constant of subgrade soil are satisfactory.
- 2) No existing model in Table 3.4 is found to be suitable for high-density materials of the base layer.
- 3) A new model has been proposed for the compacted base materials based on this study.

However, the improved TDR is still a troublesome device because of its large size and the time-consuming data processing required. The other major disadvantage is that the energy consumption of the TDR is high. Because of these drawbacks, a new Moisture Sensor (MS) system was specially developed in this study and verified in the MAT section of TxDOT. This new MS system is highly recommended by the researchers to replace the current modified TDR system in future MLS tests. A detailed introduction to this new MS system is given in Chapter 7.

### 6.2 GPR SYSTEM

Ground Penetrating Radar (GPR) can be used as a fully non-destructive device to determine the moisture content of different layers under the pavement. GPR has been shown to be one of the most useful tools for subsurface imaging due to its flexibility in operation and its capability to offer high resolution at the desired depth.

The time-domain Transmission Line Matrix (TLM) method and a Perfect Matched Layer (PML) proved to be efficient in detecting the dielectric constant of the subsurface materials and minimizing the computation space. The dielectric constant of one-dimensional structures could be reconstructed with a layer stripping technique. The one-layer and two-layer laboratory test results indicated the following:

- 1) The inversion method was efficient. Only limited proximate initiation data were required, such as the number of layers and depths of each layer to start the iterative calculation; and
- 2) The dielectric constants of sand and soils used in this study correlated well with their moisture contents.

Six groups of field data were collected. However, the field data were not satisfactory. Further field experiments will be conducted when the clarity of the waveforms can be improved.

## CHAPTER 7: RECOMMENDATIONS

### 7.1 THE NEW MOISTURE CONTENT MEASUREMENT SYSTEM

Moisture content can be measured in many ways. The TDR system gives accurate results. However, for reasons of the complexity, cost, and high power required by the TDR, the existing system is not economical and is not easy to use in practical applications. An experimental study of a new soil moisture content sensor is conducted. A parallel transmission line is developed to measure the moisture content using the phase information of the transmitted waves at 1 GHz. A sensor is built and tested. The test results show that the system improves the accuracy and is simple to use. Figure 7.1 is a set of pictures of this new device and the laboratory test environment.

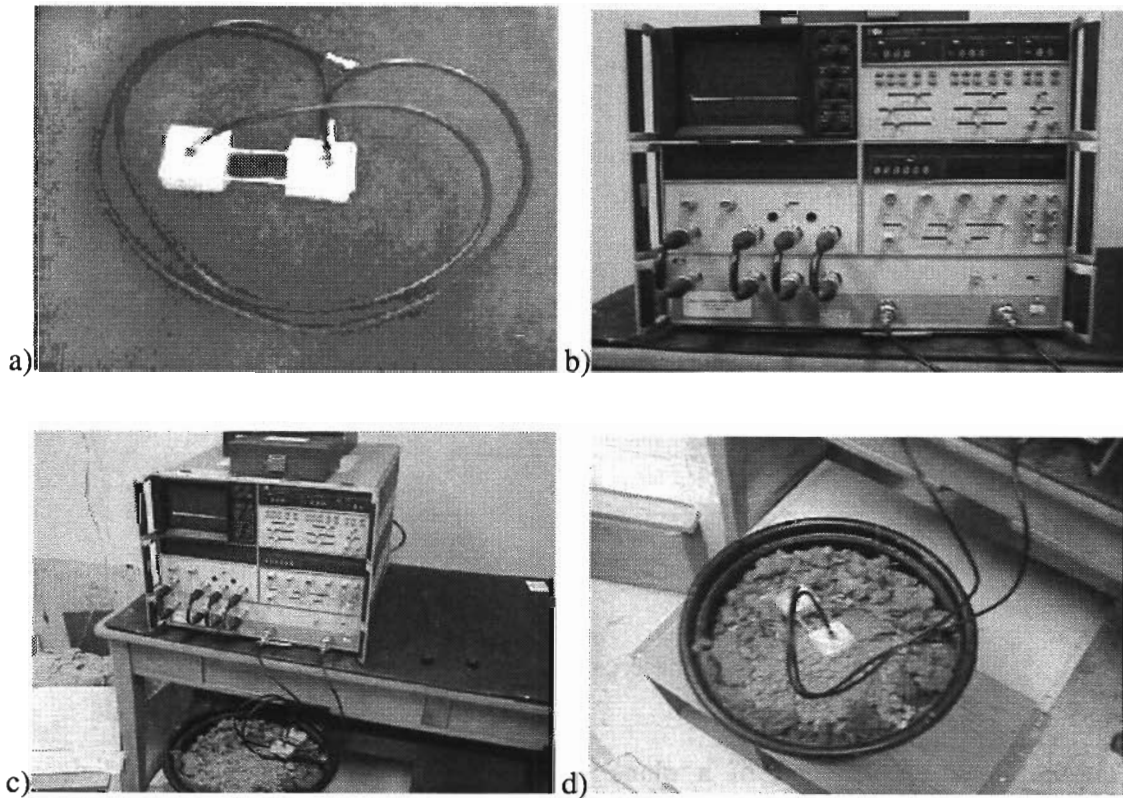


Figure 7.1 The new moisture content measurement system:

a) The MS probe b) The MS main system c) Lab test at UH d) Soil sample test

#### 7.1.1 The Basic Principle of the New Moisture Sensor

The theoretical background of this sensor is shown in Figures 7.2 and 7.3 and can be summarized as follows:

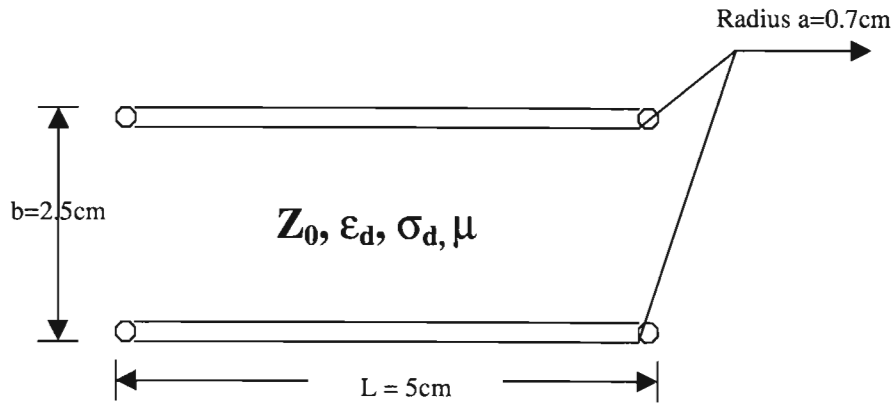


Figure 7.2 A two-wire transmission line diagram

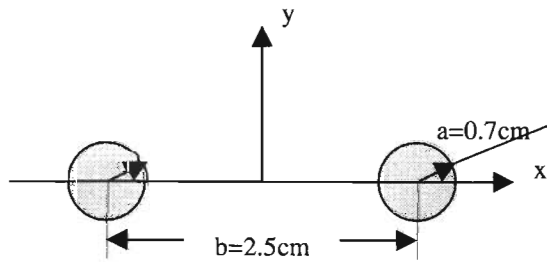


Figure 7.3 The cross-section of the sensor

The propagation constant of a plane electromagnetic wave in a lossy dielectric medium is defined as:

$$\gamma = \alpha + j\beta = j\omega\sqrt{\mu_d\epsilon_d} \quad (7.1)$$

where  $\alpha$  is the attenuation constant and  $\beta$  is the phase constant. For a nonmagnetic material, when  $\mu_d$  is equal to  $\mu_0$  and  $\epsilon_d$  is complex number, the propagation constant may be expressed as:

$$\gamma = j\frac{2\pi}{\lambda_0}\sqrt{\epsilon_r + j\sigma/\omega}. \quad (7.2)$$

The  $\beta$  component of the propagation constant can now be rewritten as:

$$\beta = \frac{2\pi}{\lambda_0} \sqrt{\frac{\epsilon_r}{2} (\sqrt{1 + \tan^2 \delta} + 1)} \quad (7.3)$$

where  $\lambda_0$  is the wavelength in free space,  $\epsilon_r$  is relative permittivity and  $\delta$  is equal to  $\sigma/\omega\epsilon_r$ . Because  $\delta$  is much less than 1 (researchers applied this formula for this experiment at 1 GHz frequency), Eq. (7.3) can be simplified to the following:

$$\beta = \frac{2\pi}{\lambda_0} \sqrt{\epsilon_r} = 20.944 \sqrt{\epsilon_r} \quad (7.4)$$

So,

$$\theta = \beta l = \frac{2\pi}{\lambda_0} l \sqrt{\epsilon_r} = \theta_0 \sqrt{\epsilon_r} \quad (7.5)$$

The phase difference  $\theta$ , between the two wires is a function of relative permittivity of the medium between them. Since the relative permittivity is related to the moisture content of the medium, the moisture change results in the phase change.

### 7.1.2 Laboratory Tests at UH

#### Test Conditions

- 1) HP 8505A Network Analyzer: used to measure the phase of the transmitted wave.
- 2) The new moisture sensor: the transmission line consists of a pair of 5 cm long, 0.7 cm radius, circular-cross-section parallel bronze wires, two transformers, and associated microstripline matching networks. The distance between the two axes of the wires is 2.5 cm.
- 3) Electronic and mechanical precision scales are used for the tests.
- 4) Test samples are sand and soil obtained from the UH campus.

#### Test Procedures

- 1) Dry the sample in the oven;
- 2) Measure the phase  $\theta_0$  in air and set it as the HP 8508A's reference;
- 3) Measure the phase  $\theta_d$  of the dry sample;
- 4) Add 2% of water;
- 5) Stir the mixture for 5 minutes;
- 6) Measure the phase  $\theta_w$  of moist sample; and
- 7) Repeat from step 4 until the phase water content is 20%.

### Data and Analysis

In the dry sand,  $\theta_0 = \beta b = 2\pi b/\lambda_0 = 32^\circ$ . The data are listed in the Table 7.1 and plotted in Figure 7.4.

*Table 7.1 Data measured during two experiments for sand and soil samples*

Weight Moisture Content (%)	Phase (Degree) Soil	Phase (Degree) Sand
0	-33	-31
1		-33
2	-38	-38
3		-41
4	-51	
5		-49
6	-58	
7		-58
8	-68	
9		-67
10	-83	
11		-77
12	-98	
13		-83
14	-105	
15		-95
16	-113	
17		-138
18	-160	
19		-154

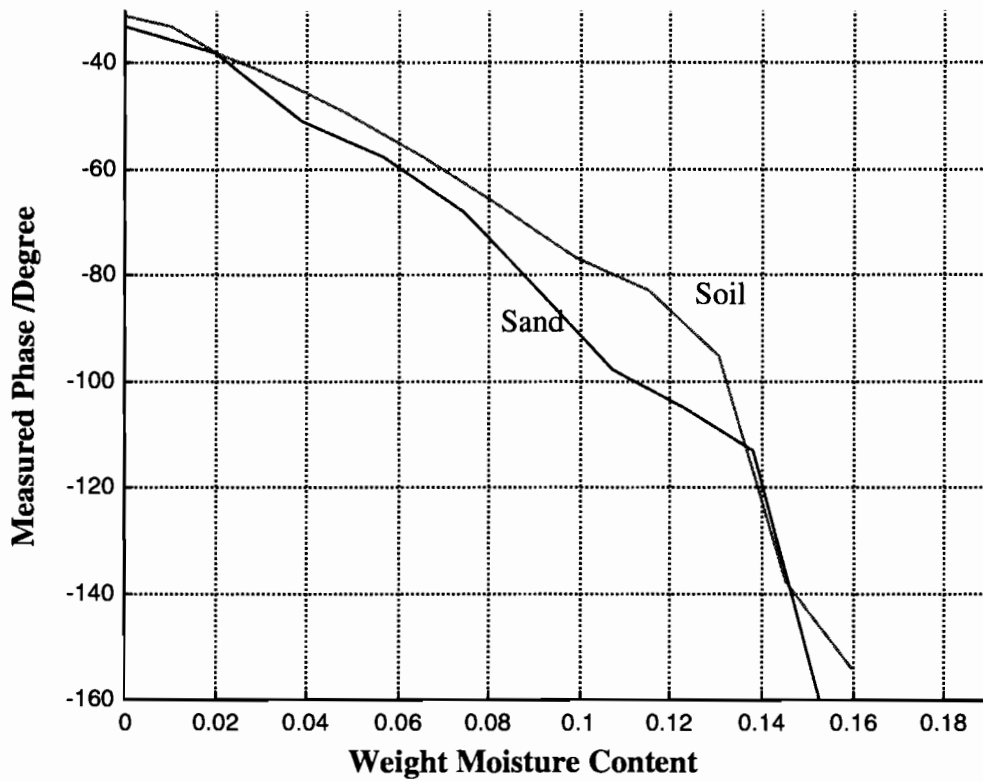


Figure 7.4 Phase vs. weight moisture content

### 7.1.3 Laboratory Tests at TxDOT Materials Lab

This device was brought to the TxDOT materials lab for evaluation. Three different materials were used during the tests: sand, soil, and aggregates. The tested moisture content ranged from 0% to about 20% (saturated). The measured accuracy reached 1%.





## **APPENDIX**

As mentioned in Chapter 2, two systems were developed for the different purposes; one for laboratory study and the other for field measurement.

### **A.1 SYSTEM I: SYSTEM FOR THE LABORATORY MEASUREMENT OF SOIL MOISTURE CONTENT**

In this system, a computer controls the TDR directly using the SP232 Serial Extended Function Module (EFM) which follows the RS232-C serial protocol [34]. This system is developed to acquire waveforms and use them to compare with simulation results. System I only measures data from one soil sample at a time. However, this system is not fully described in this report.

### **A.2 SYSTEM II: SYSTEM FOR THE IN-SITU MEASUREMENT OF SOIL MOISTURE CONTENT**

This system is developed for the Texas Department of Transportation (TxDOT) for the in-situ measurement of soil moisture content. At the test sites of US281 (southbound and northbound), Jacksboro, Texas, the weather records from a weather station system are automatically read through the developed CR10 datalogger. Using this modified datalogger allows us to automatically control and monitor the TDR readings and measurements. The datalogger works very efficiently since it contains the Programmable Read Only Memory (PROM) instructions that can control the sequence of the measurement, apply the mathematical algorithms for calculating moisture content and electrical conductivity, store the resulting data, and link to a computer for the data and program transfer. The volume moisture contents of the soil from eight different points at each test site were measured at the same time through a multiplexer (SM406).

### **A.3 TDR HARDWARE SYSTEM**

The TDR hardware for the field test and measurement of the soil moisture content is developed in this study. By using this equipment instead of manually recording the data, this PROM datalogger greatly improves the efficiency and the integrity of data processing.

#### **A.3.1 Introduction of the System**

With this improved system, the modified datalogger controls the measurement sequence, applies mathematical algorithms for calculating the moisture content and the electrical conductivity, stores the data, and links to a computer for data and program transfer [35-36]. The schematic diagram of this system is shown in Figure A1. The reflectometer used in this system is the Tektronix 1502B TDR Cable Tester equipped with Campbell Scientific's SDM1502 Communications Interface and PS1502B Power Control Module. The CR10 Datalogger has a serial communication port and is

connected to a Personal Computer using a modem. The multiplexer SDM50 is an eight-to-one 50 ohm co-axial multiplexer, and the eight probes are connected to the SMD50's 8 input ports.

In this research project, seven thermocouples were also installed into the modified datalogger to automatically measure the soil temperature at seven different underground positions. Because the original datalogger used for the weather station does not have Programmable Read-Only-Memory (PROM) for the special functions required for TDR measurements, a modified datalogger with PROM replaced the original one.

Some wiring in the CR10 datalogger had to be modified for the additional new wires in the TDR system. These modifications also required changes to the software, but had no effect on the original function or performance of the weather station.

The original program is also revised to allow the thermocouples and TDR system to measure the temperature and moisture content of soil, respectively.

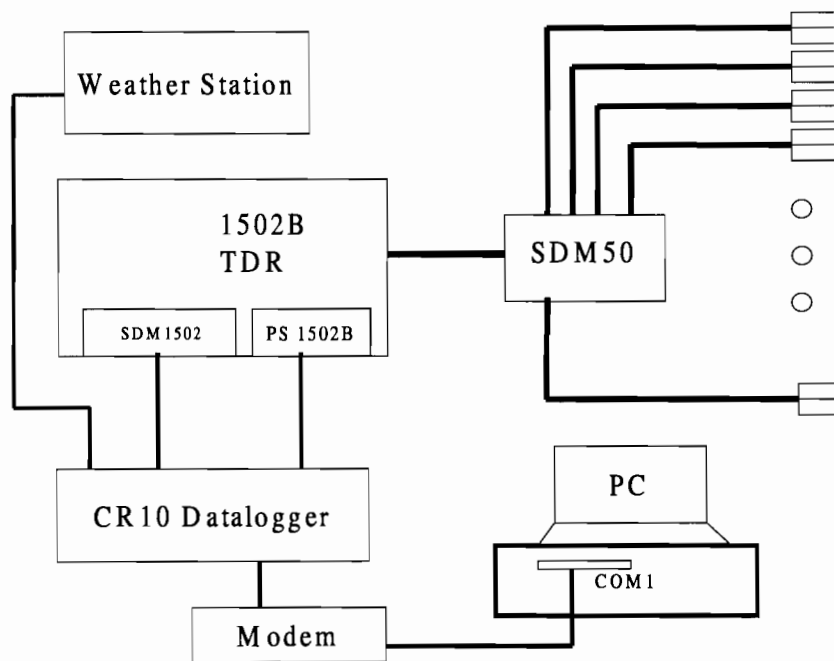


Figure A1 Schematic of the modified CR10 datalogger for the TDR system

### A.3.2 Hardware Components

#### Datalogger

The modified CR10 datalogger controls the sequence of the measurement, applies mathematical algorithms to calculate moisture content and electrical conductivity of

material / soil, stores the target data and links to a computer for data and program transfer.

For these special function requirements, a PROM component is added to the datalogger. A large amount of programming work has been done to meet the requirements of the project, such as adding new wires and writing new instructions. The details of the programming were very lengthy. From a civil engineering point of view, these instruction codes, protocols, and algorithms are too specific to comprehend, and thus, the major portion of the development is omitted in the report.

### **1502B TDR Cable Tester**

The 1502B is a cable tester manufactured by Tektronix. In the application of Time Domain Reflectometry (TDR) for soil moisture content measurements, the 1502B is the source of a very short rise-time pulse which applies to a waveform on a lithium crystal display, and digitizes the waveform for output.

### **SDM1502 Communication Interface**

The SDM1502 (Synchronous Device for Measurement) is plugged into the front panel of the 1502B and performs the necessary communication interface functions to transfer the 1502 control instructions and the data between the 1502B and the datalogger. A 5-wire connector on the SDM1502 front panel provides 2 lines for 12-volt DC power and 3 lines for synchronous communications.

The use of synchronous communication requires adherence to an addressing scheme for the communication devices. The address of the SDM1502 is selected using a dip-switch with 4 two-position switches. The address value used for the SDM 1502 to dictate the address must be used for the multiplexers (SDM50). There is a maximum of three hierarchical multiplexer levels.

### **PS1502B Control Module**

The PS1502B module allows the datalogger to control the sequence when the power is applied to the 1502B. A 3-wire connector passes 12-volt DC and a control line from the datalogger. Turning on the 1502B only during the measurements can provide significant power savings when there is limited power available. Additionally, the 1502B initializes control settings upon power-up and will reset any faults that might otherwise result in loss of data.

### **SDM50 Multiplexer**

The SDM50 is an eight-to-one 50 ohm co-axial multiplexer with BNC connectors. The co-axial cable coming from the 1502B connects to the common terminal. Spark gaps provide protection from voltage surge damage. Each of the eight ports can be connected to a probe or another multiplexer.

The multiplexers use synchronous communication and require an address coordination with the SDM1502 module. The address of the multiplexer is set by positioning jumpers on the circuit board. The wiring diagram of the multiplexer communication cables from the SDM1502 and SDM50 to the datalogger is shown in Figure A2.

## **Probes and Cables**

These probes are unbalanced, each having three rods. A central rod is connected to the signal lead of the co-axial cable. The other rods are arranged radially around the center and are connected to the shield of the co-axial cable. The advantages of this unbalanced probe are that they are smaller than with balanced design, and that measurements are concentrated around the central electrode.

## **Wiring**

The terminals labeling 1H through 6H are analogy inputs that can be used as differential or Single-Ended (SE) inputs, depending on the sensor configuration. When used as a differential input, voltage on the H input is measured with respect to voltage on the L input. SE channels 1 through 12 were labeled "SE". When used as an SE input, the voltage was measured with respect to Analogy Ground (AG). The output ports (COM L1 and H1) of the thermocouple multiplexer are configured as differential inputs and connected to 6H and 6L. Figure A3 shows the wiring of the thermocouples.

## **A.4 SOFTWARE TOOLS**

### **PC208E Support Software**

The PC208E software package consists of several separate packages. PC208E provides computer / datalogger communication for data collection and real-time data display. It also provides tools to set the datalogger clock, transfer datalogger programs and test communication links [36].

### **Edlog**

Edlog is a program used to create and edit datalogger programs on the PC. Compiled programs may then be transferred to the datalogger over a telecommunication link using the PC208E.

### **Programming the CR10**

The CR10 datalogger must be programmed before it can make any measurements. A program consists of a group of instructions entered into a program table [37-38]. The program table is given an executable interval that determines how frequently that table is executed. When the table is executed, the instructions are executed in sequence from beginning to end. After executing the table, the CR10 waits for the remainder of the execution interval, and then executes the table again.

The interval at which the table is executed generally determines the interval at which the TDR probes are measured. The interval at which the data are processed and stored is separate from the interval of table execution, and may vary from samples. An execution interval may vary millisecond to an hour, a day, or have irregular intervals. The output interval is determined by how often the output flag is set to high. Figure A4 shows the program procedure and structures.

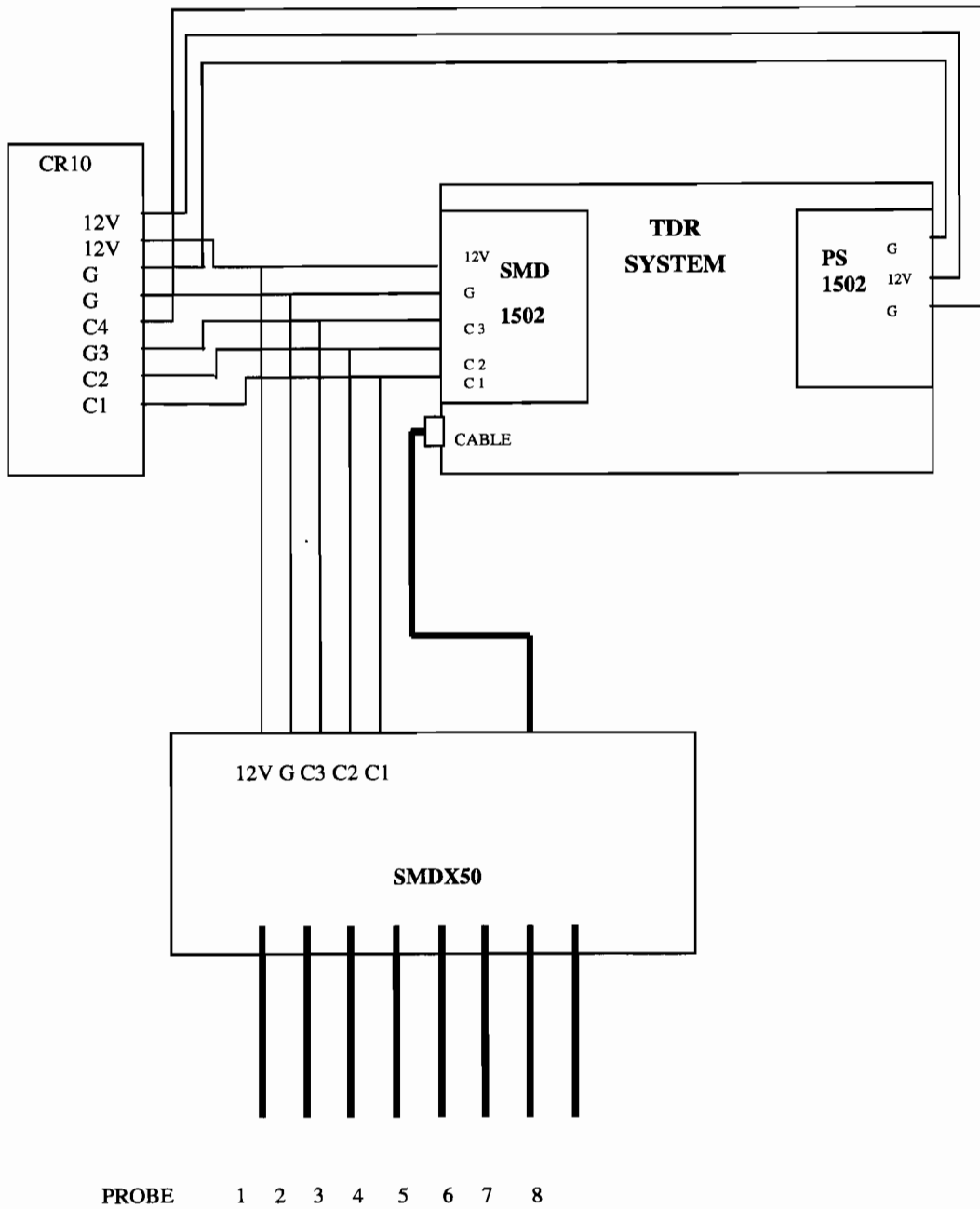


Figure A2 Wiring diagram of the multiplexer communication cables from the SDM1502 and SDM50 to the datalogger

AM416 RELAY MULTIPLEXER

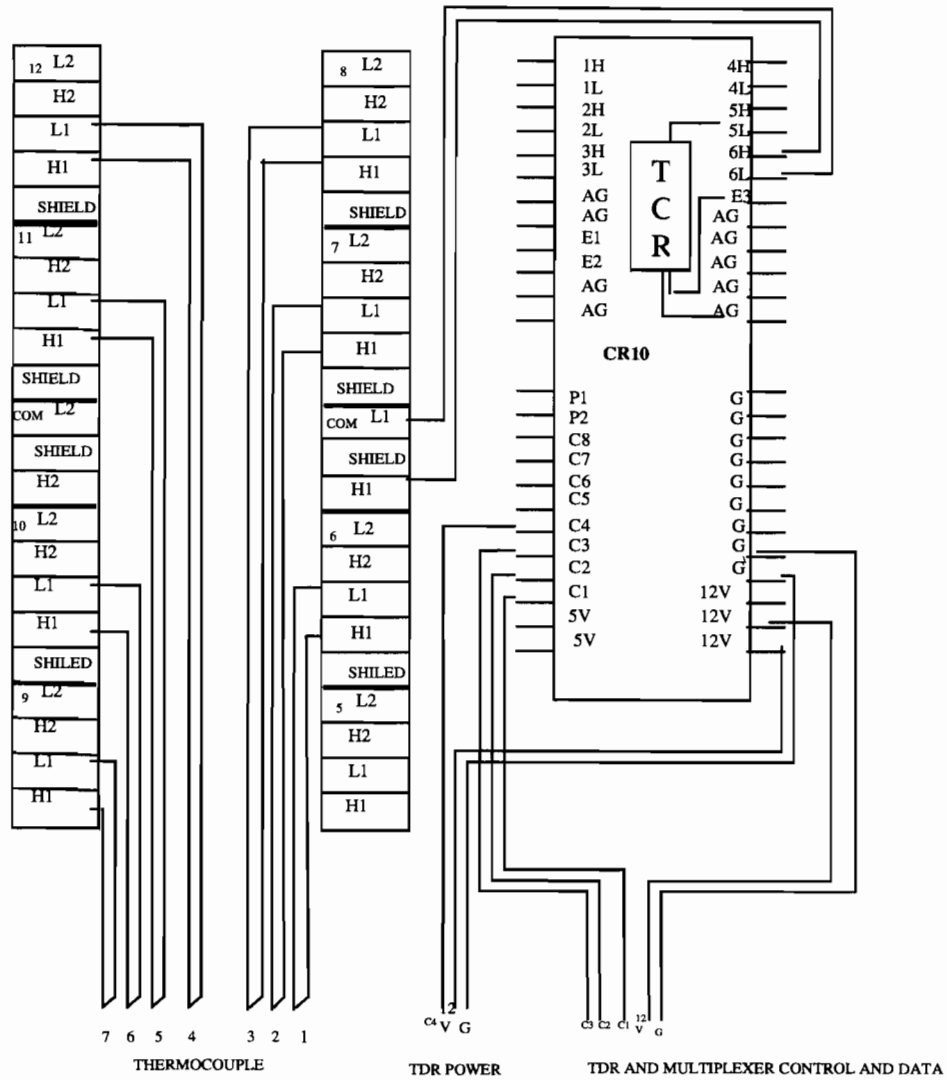


Figure A3 Datalogger wiring for the TDR (left part of this figure is the thermocouples installed at US281, Jacksboro, Texas)

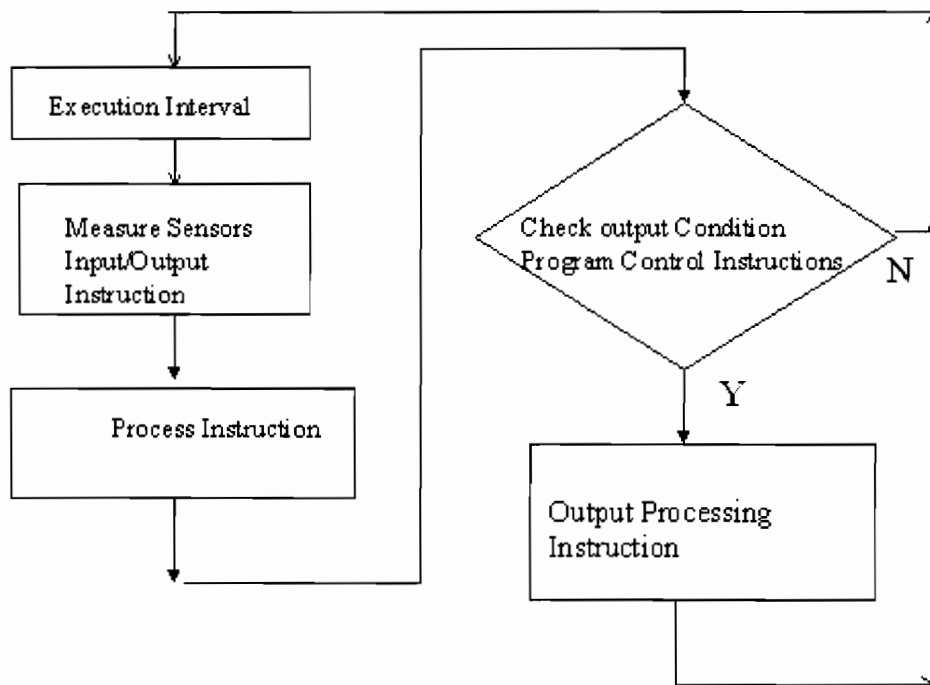


Figure A4 Program flow chart





## REFERENCES

- [1] J. Klemunes, Jr., "Determining Soil Volumetric Moisture Content Using Time Domain Reflectometry," FHWA-RD-97-139.
- [2] S. I. Siddiqui and V. P. Drnevich, "A New Method of Measuring Density and Moisture Content of Soil Using the Technique of Time Domain Reflectometry," FHWA/IN/JHRP-95/9.
- [3] J. Ledieu, P. De Ridder, P. De Clerck and S. Dautrebande, "A Method of Measuring Soil Moisture by Time-Domain Reflectometry," *Journal of Hydrology*, 88 (1986), pp. 319-328.
- [4] G. C. Topp, J. L. Davis and A. P. Annan, "Electromagnetic Determination of Soil Water Content: Measurements in Coaxial Transmission Lines," *Water Resources Research*, Vol. 16, No. 3, June 1980, pp. 574-582.
- [5] C. Liu and L. C. Shen, "Dielectric Constant of Two-Component, Two-Dimensional Mixtures in Terms of Bergman-Milton Simple Poles," *Journal of Applied Physics*, Vol. 73, No. 4, 15 February, 1993.
- [6] C. Liu and H. Wu, "Computation of the Effective Dielectric Constant of Two-Component, Three-Dimensional Mixtures Using a Simple Pole Expansion Method," *Journal of Applied Physics*, Vol. 82, No. 1, 1 July 1997.
- [7] J. R. Wang and T. J. Schmugge, "An Empirical Model for the Complex Dielectric Permittivity of Soil as a Function of Water Content," NASA Tech. Memo. 79659, Goddard Space Flight Center, Greenbelt, Md., 1978, p. 35.
- [8] J. E. Hipp, "Soil Electromagnetic Parameters as a Function of Frequency, Soil Density and Soil Moisture," *Proc. IEEE*, Vol. 62, 1974, pp. 98-103.
- [9] P. Hoekstra and A. Delaney, "Dielectric Properties of Soils at UHF Microwave Frequencies," *J. Geophys. Res.*, Vol. 79, 1974, pp. 1969-1706.
- [10] D. M. Pozar, *Microwave Engineering*, Addison-Wesley, Inc. 1990.
- [11] P. C. Magnusson, G. C. Alexander and V. K. Tripathi, "Transmission Lines and Wave Propagation," 3rd Edition, CRC Press, Inc., 1992.
- [12] D. Wobschall, "A theory of the Complex dielectric Permittivity of Containing Water: the semi-disperse model," *IEEE Trans. Geosci. Electron*, Vol. 15, 1977, pp. 49-58.
- [13] S. S. Smith and T. Scullion, "Development of Ground-Penetrating Radar Equipment for Detecting Pavement Condition for Preventive Maintenance," Strategic Highway Research Program, SHRP-H-672, October 1993.
- [14] C. Liu and D. H. Chen, "A Theoretical Approach to Predict Water Content from Effective Dielectric Constant of Soil Using a Simple Pole Expansion Method," *Geophysical Prospecting*, submitted October 1998.

- [15] B. M. Das, "Advanced Soil Mechanics," International Edition, McGraw-Hill Book Company, 1985, p. 9.
- [16] F. Hugo, D. H. Chen, K. Fults, A. Smit, and J. Bilyeu, "An Overview of the TxMLS Program and Lessons Learned," Proceeding, CD-ROM, 1<sup>st</sup> International Conference on Accelerated Pavement Testing. Reno, Nevada. October 18-20, 1999.
- [17] D. H. Chen, J. Bilyeu, and R. He, "Comparison of Resilient Moduli Between Field and Laboratory Testing: A Case Study," Presented at the 78<sup>th</sup> Annual Transportation Research Board Meeting. Paper #990591, Washington D. C., January 10-14, 1999.
- [18] T. Scullion, C. L. Lau, and Y. Q. Chen, "Implementation of the Texas Ground Penetration Radar System," Texas Transportation Institute, Research Report 1233-1, p. 1.
- [19] C. Liu and L. C. Shen, "Response of Electromagnetic-pulse Logging Sonde in Axially Symmetrical Formation," IEEE Transactions on Geoscience and Remote Sensing, Vol. 29, No. 2, March 1991, pp. 214-221.
- [20] N. R. S. Simons, A. R. Sebak, and G. E. Bridges, "Application of the TLM Method to Half-Space and Remote-Sensing Problems," IEEE Transactions on Geoscience and Remote Sensing, Vol. 33, No. 3, May 1995, pp. 759-767.
- [21] C. Liu and L. C. Shen, "Numerical Simulation of Subsurface Radar for Detecting Buried Pipes," IEEE Transactions on Geoscience and Remote Sensing, Vol. 29, No. 5, September 1991, pp.795-798.
- [22] W. J. R. Hoefler, "The Transmission Line Matrix Method-Theory and Applications," IEEE Transactions. Microwave Theory tech. Vol. 33, 1985, pp. 882-893.
- [23] Z. Wu, "An Image Reconstruction Method Using GPR Data," Department of Electrical and Computer Engineering, University of Houston, Houston, Texas.
- [24] C. C. Lin, and K. K. Mei, "Time Domain Absorbing Boundary Condition in Lossy Media," IEEE Transactions. Nucl. Sci. 30, 1983, pp. 4583-4588.
- [25] Y. M. Zhang and C. Liu, "A Space Marching Inversion Algorithm for Pulsed Borehole Radar in the Time-Domain," IEEE Transactions. Geoscience and Remote Sensing, Vol.33, 1995, pp. 541-550.
- [26] W. M. Boerner, A. K. Jordan, and I. W. Kay, "Introduction to the Special Issue on Inverse Methods in Electromagnetics," IEEE transactions. Antennas Propagating. Vol. AP-29, March, 1981, pp. 185-189.
- [27] M. Moghaddam and W. C. Chew, "Non-Linear Two-Dimensional Velocity Profile Inversion Using Time Domain Data," IEEE Transactions. Geoscience and Remote Sensing, Vol.30, January. 1992, pp.147-156.

- [28] J. P. Warhus, J. E. Mast, E. M. Johansson, and S. D. Nelson, "Advanced Ground Penetrating Radar," Lawrence Livermore National Laboratory, Electronics Engineering Department.
- [29] S. Xie, D. Lan, J. Wang, Y. Zhang, R. Liu, and D. Shattuck, "The Development of an Advanced GPR System at the University of Houston," Proceedings of the Fifth International Conference on Ground Penetrating Radar, Kichener, Ontario, Canada, 1994, pp. 1091-1100.
- [30] J. L. Davis and A. P. Annan, "Ground Penetrating Radar for High-Resolution Mapping of Soil and Rock Stratigraphy," *Geophysical Prospecting* 37, 1988, pp. 531-551.
- [31] D. J. Daniels, D. J. Gunton and H. F. Scott, "Introduction to Subsurface Radar," *IEE Proceedings*, Vol. 135, 1988, pp. 278-328.
- [32] D. R. Inkster, J. R. Rossiter, R. Goodman, M. Galbraith and J. L. Davis, "Ground Penetrating Radar for Subsurface Environmental Application," Presented at the Seventh Thematic Conference on Remote Sensing for Exploration Geology, Calgary, Alberta, Canada, October 2-6, 1989.
- [33] S. Xie, "Ground Penetrating Radar Transmitter and Receiver Design," M.S. Thesis, University of Houston, December, 1994.
- [34] Instruction Manual, SP232 Serial Extended Function Module (for 1502B, 1503B MTDRs), Tektronix, Inc.
- [35] Instruction Manual, PC208E Support Software, Campbell Scientific, Inc.
- [36] Instruction Manual, CR10 Training Manual, Campbell Scientific, Inc.
- [37] H. T. Lau, *Numerical Library in C for Scientists and Engineers*, CRC Press, Inc., 1995.
- [38] J. M. Baker and R. R. Allmaras, "System for Automating and Multiplexing Soil Moisture Measurement by Time Domain Reflectometry," *Soil Society of America Journal* 54, pp. 1-6, 1990.